

DESIGN, FABRICATION, AND STATIC TESTING OF FIRST-STAGE
ATTACHED INFLATABLE DECELERATOR (AID) MODELS

By B. A. Johnson

Prepared under Contract No. NAS1-10105 by
GOODYEAR AEROSPACE CORPORATION
Akron, Ohio

for

Langley Research Center
NATIONAL AERONAUTICS AND SPACE ADMINISTRATION

FOREWORD

Work described in this document was performed by Goodyear Aerospace Corporation, Akron, Ohio, under NASA Contract NAS1-10105. The contractor's number for this report is GER-15267.

CONTENTS

	<u>Page</u>
FOREWORD.	iii
ILLUSTRATIONS	vii
TABLES.	xi
<u>TITLE</u>	
SUMMARY	1
INTRODUCTION.	1
SYMBOLS	2
AID MODEL DESCRIPTION	5
DESIGN CONDITIONS	7
Shape Analysis.	7
Canopy Gore Patterns.	10
Inlet Sizing.	16
SYSTEM DESIGN	16
Forward Inlets.	16
Aft Inlets.	17
Canopy Attachment Scheme.	21
Canopy Storage and Release.	21
MODEL INSTRUMENTATION	21
PIVOTAL BALANCE ADAPTER	24
MATERIAL SELECTION.	25
Hard Structure.	25
Fabric.	27
DEVELOPMENT TESTS	29
General	29
Tensile Tests of Nomex Fabric	29

	<u>Title</u>	<u>Page</u>
Fabric Permeability Tests.		30
Deployment and Inflation Test.		30
CONCLUSIONS.		31
<u>Appendix</u>		
A	DRAWINGS	35
B	STRESS ANALYSIS.	91
C	WEIGHT ANALYSIS.	93
REFERENCES		97

ILLUSTRATIONS

<u>Figure</u>	<u>Title</u>	<u>Page</u>
1	Drag Performance of AID and Disk-Gap-Band Parachute.	3
2	Variations in Decelerator Mass and Landed Payload Mass with Ballistic Coefficient	3
3	Details of Model I Configuration	6
4	Details of Model II Configuration.	6
5	Cutaway Drawing of an AID.	8
6	Analytical Pressure Distribution for Model I . .	9
7	Analytical Pressure Distribution for Model II. .	9
8	Model I Gore Pattern	15
9	Model II Gore Pattern.	15
10	Forward Inlet Spring Attached to Hard Structure.	17
11	Forward Inlet Spring Position.	18
12	Forward Inlet Sketch	19
13	Relative Angular Displacement of Inlets (Looking Downstream	20
14	Canopy Attachment Scheme	22
15	Canopy Stowage and Release Scheme.	23
16	AID Model in Packaged Configuration.	24
17	Load Cell Attachment to Meridian	25
18	Serial Numbers and Location of Load Cells for Each Model	26
19	Sketch of Pivotal Adapter.	27
20	Test Setup for Static Test of Pivotal Adapter. .	28
21	Water-Alcohol Inflation Test Setup	32

Figure	Title	Page
22	AID Differential Pressure-Time History.	33
23	Load Cell Force-Time History.	33
24	Fully Inflated AID.	34
A-1	Attached Inflatable Decelerator System - Drawing 3063000-001, Sheet 1.	37
A-2	Attached Inflatable Decelerator System - Drawing 3063000-001, Sheet 2.	39
A-3	Attached Inflatable Decelerator System - Drawing 3063000-001, Sheet 3.	41
A-4	Attached Inflatable Decelerator System - Drawing 3063000-001, Sheet 4.	43
A-5	Attached Inflatable Decelerator System - Drawing 3063000-001, Sheet 5.	45
A-6	Decelerator Assembly, Attached Inflatable - Drawing 3063000-002, Sheet 1.	47
A-7	Decelerator Assembly, Attached Inflatable - Drawing 3063000-002, Sheet 2.	49
A-8	Decelerator Assembly, Attached Inflatable - Drawing 3063000-002, Sheet 3.	51
A-9	Decelerator Assembly, Attached Inflatable - Drawing 3063000-002, Sheet 4.	53
A-10	Decelerator Assembly, Attached Inflatable - Drawing 3063000-002, Sheet 5.	55
A-11	Decelerator Assembly, Attached Inflatable - Drawing 3063000-002, Sheet 6.	57
A-12	Decelerator Assembly, Attached Inflatable - Drawing 3063000-002, Sheet 7.	59
A-13	Decelerator Assembly, Attached Inflatable - Drawing 3063000-002, Sheet 8.	61
A-14	Decelerator Assembly, Attached Inflatable - Drawing 3063000-002, Sheet 9.	63
A-15	Decelerator Assembly, Attached Inflatable - Drawing 3063000-002, Sheet 10	65

<u>Figure</u>	<u>Title</u>	<u>Page</u>
A-16	Support Ring Assembly and Aeroshell, Attached Inflatable Decelerator System - Drawing 3063000-003, Sheet 1.	67
A-17	Support Ring Assembly and Aeroshell, Attached Inflatable Decelerator System - Drawing 3063000-003, Sheet 2.	69
A-18	Support Ring Assembly and Aeroshell, Attached Inflatable Decelerator System - Drawing 3063000-003, Sheet 3.	71
A-19	Support Ring Assembly and Aeroshell, Attached Inflatable Decelerator System - Drawing 3063000-003, Sheet 4.	73
A-20	Support Ring Assembly and Aeroshell, Attached Inflatable Decelerator System - Drawing 3063000-003, Sheet 5.	75
A-21	Support Ring Assembly and Aeroshell, Attached Inflatable Decelerator System - Drawing 3063000-003, Sheet 6.	77
A-22	Support Assembly, Attached Inflatable Decelerator - Drawing 3063000-004, Sheet 1.	79
A-23	Support Assembly, Attached Inflatable Decelerator - Drawing 3063000-004, Sheet 2.	81
A-24	Support Assembly, Attached Inflatable Decelerator - Drawing 3063000-004, Sheet 3.	83
A-25	Support Assembly, Attached Inflatable Decelerator - Drawing 3063000-004, Sheet 4.	85
A-26	Spring and Ring Assembly, Decelerator Assembly, Attached Inflatable - Drawing 3063000-110, Sheet 1	87
A-27	Tube Assembly, Decelerator Assembly - Drawing 3063000-112, Sheet 1.	89
C-1	Reference Datum for AID Models Mounted on Pivotal Adapter	93
C-2	Reference Datum for AID Models Without Pivotal Adapter	94

TABLES

<u>Table</u>	<u>Title</u>	<u>Page</u>
I	AID Model Designation.	5
II	AID Design Conditions.	7
III	AID Canopy Parameters.	8
IV	AID Coordinates for Model I.	11
V	AID Coordinates for Model II	12
VI	Model I Lobe Geometry, Radial Growth Due to Unrestrained Thread Packing, and Fabric Stressess. . . .	13
VII	Model II Lobe Geometry, Radial Growth Due to Unrestrained Thread Packing, and Fabric Stresses	14
VIII	AID Inlet Sizes.	16
IX	Tensile Strength Test Results of Canopy Fabric . . .	30
C-I	AID Models Weight Breakdown.	94
C-II	AID Models Center of Gravity Locations	95

DESIGN, FABRICATION, AND STATIC TESTING
OF FIRST-STAGE
ATTACHED INFLATABLE DECELERATOR (AID) MODELS

By B. A. Johnson
Goodyear Aerospace Corporation

SUMMARY

Goodyear Aerospace Corporation (GAC) designed and fabricated wind-tunnel models of a first-stage Attached Inflatable Decelerator (AID) for the NASA Langley Research Center (LRC).

Six models were furnished by GAC for the current program. The AID canopies were attached directly to a payload in a method which simulated a first-stage AID. All six models had 140-deg conical aeroshells as their forebodies, and each model had four spring-actuated forward inlets mounted on the internal hard structure to provide for initial deployment. Full inflation and final pressurization is accomplished by four aft canopy inlets on each model.

An inflation test was conducted in an environmental chamber to investigate packaging, deployment, and inflation characteristics of the models prior to wind-tunnel testing.

INTRODUCTION

Recent advancements in high-speed flight vehicles have established the need for a deceleration system with good operational characteristics at supersonic speeds. To meet this need, LRC has conducted extensive analytical and experimental investigations in the development of an Attached Inflatable Decelerator (AID), the results of which are summarized in References 1 through 10. An AID consists of a flexible canopy deployed and inflated by ram air, which is attached to the base of the body to be decelerated. AID models investigated to date (References 1 through 10) were representative of a single-stage decelerator in which the deployed drag area was sufficient to decelerate the payload to terminal conditions suitable for descent engine ignition.

A recent trade-off study was conducted by LRC (References 1 and 11) to determine the effects of a two-stage deceleration system on mission performance. This system maximized decelerator efficiency by taking advantage of the high supersonic drag of

the AID as the first-stage and the high subsonic drag of a terminal-stage parachute such as the disk-gap-band parachute (Figure 1). Reference 1 states that for entry into the low-density atmosphere of Mars, the AID will relax the stringent deployment conditions on the parachute and will provide significant increases in landed payload mass without increasing the size of the basic aeroshell (see Figure 2). Complimenting this Reference 1 study was a parametric thermal and stress analysis of an AID operating in the most severe of the postulated Mars atmospheres (Reference 12) which showed the feasibility of deploying an AID at high supersonic speeds.

As part of a continuing effort to develop and to evaluate the AID, the present program investigated the characteristics of a first-stage AID. Since the AID is aerodynamically shaped, its canopy may be tailored to the application for which it is intended and to the attachment locations available. Key factors in this program were the investigation of a new canopy shape and a new attachment scheme. The AID models incorporated smaller volume canopies than those models described in References 3, 9 and 12 and were attached to a simulated payload in a manner which would permit detachment of the AID and deployment of a subsonic parachute rather than being attached directly to the 140-deg aeroshells. Thus, the objectives of the investigation were to design, fabricate, and static test AID models in preparation for wind-tunnel testing which will demonstrate deployment and aerodynamic performance at supersonic speeds.

SYMBOLS

B	ballistic coefficient, slugs/sq ft
C_D	drag coefficient
c_p	pressure coefficient, $p_L - P_\infty / q_\infty$
D	diameter, ft
d_g	depth of lobes, in.
F	circumferential membrane stress coefficient
f	fabric stress, lb/in.
\bar{f}	nondimensional fabric stress
f_c	circumferential fabric stress resultant, lb/in.
f_m	meridional fabric stress resultant, lb/in.

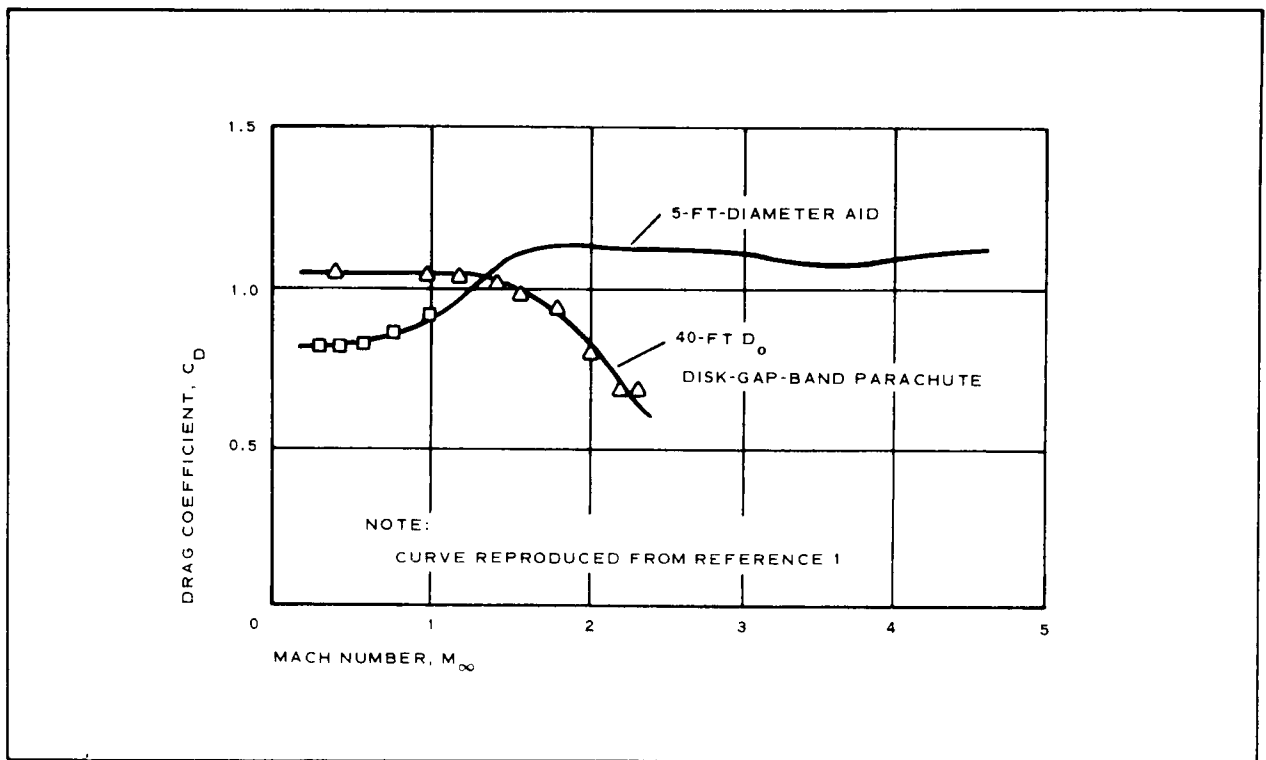


Figure 1. - Drag Performance of AID and Disk-Gap-Band Parachute

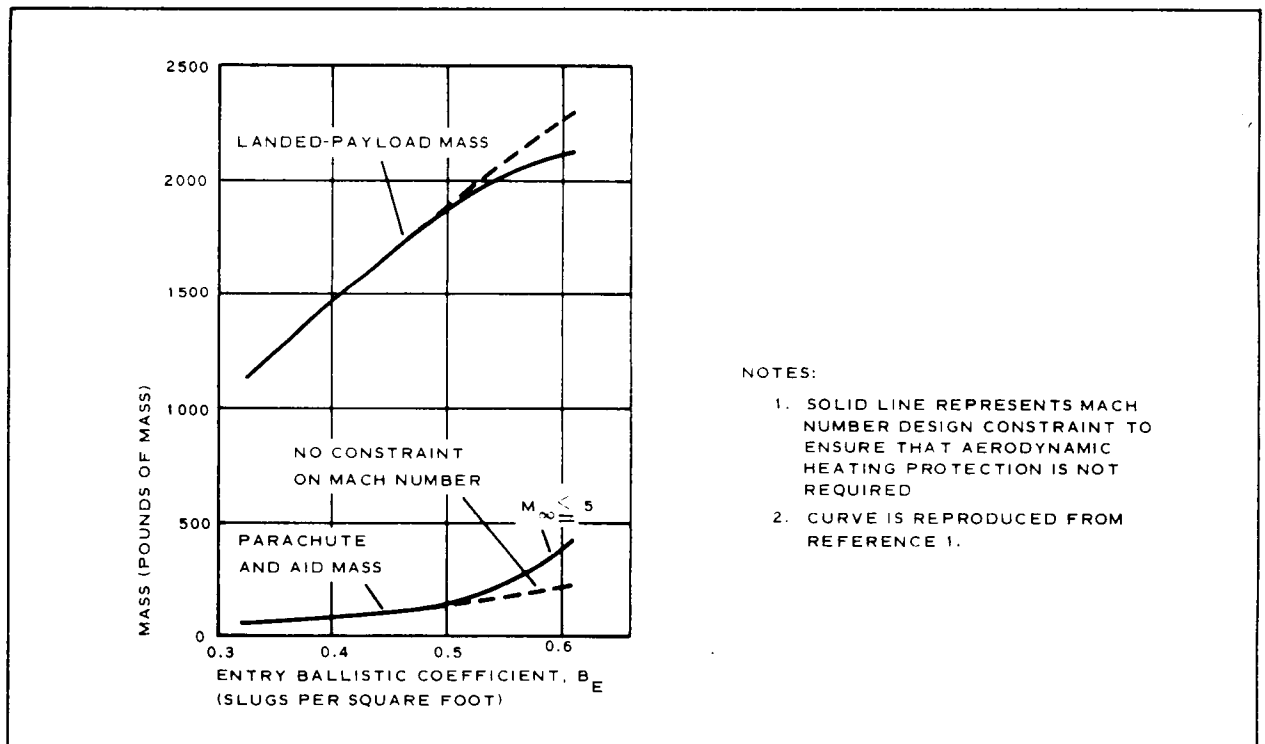


Figure 2. - Variations in Decelerator Mass and Landed-Payload Mass with Ballistic Coefficient

M	Mach number
N	stress, lb/in.
n	number of gores
p	$p_i - p_b$, psf
q	dynamic pressure, psf
R	maximum canopy radius excluding burble fence, in.
r	aeroshell base radius, in.
r_g	lobe radius, in.
S_g	half-arc length of lobe, in.
T	tension, lb
\bar{T}	nondimensional meridional tape load
x/R, y/R	decelerator coordinate shaping factors
β	central half-lobe angle, deg
γ	burble fence load carried by front surface fabric, percent; bias thread set angle, deg
ϵ	strain due to thread racking, in./in.

Subscripts

B	burble fence
b	base
E	entry
f	forward
i	internal
L	local
m	meridian
o	nominal
r	rear
∞	free stream

θ circumferential direction of surface element
 ϕ meridional direction of surface element

AID MODEL DESCRIPTION

The configuration details of each of the six models discussed in this report are shown in Figures 3 and 4. Additional design details of the models described in these two figures are presented in assembly Drawings 3063000-001-101, -103, -105, -107, -109, and -111. Table I presents a correlation of model numbers with assembly numbers. The model numbers will be used in any future reference made to the specific details of the models. A complete set of drawings for the models is presented in Appendix A.

TABLE I. - AID MODEL DESIGNATION

Model Number	Assembly Number
IA	3063000-001-101
IB	3063000-001-109
IC	3063000-001-105
ID	3063000-001-111
IIA	3063000-001-103
IIB	3063000-001-107

The models shown in Figures 3 and 4 use ram air for deployment and pressurization. Spring-actuated inlets, similar to those used on the model in Reference 6, provide the initial and restraining forces to align the forward inlets with the air flow. All six models' forward inlets are 2.5 in. in diameter. Models 1A, IC, IIA, and IIB have 2.5-in. diameter aft inlets; models IB and ID have 1.8-in. diameter aft inlets.

All model I configurations have a burble fence extension which increases the maximum decelerator diameter by 10 percent. The model II configurations differ from model I by the absence of a burble fence and the resulting change in shape.

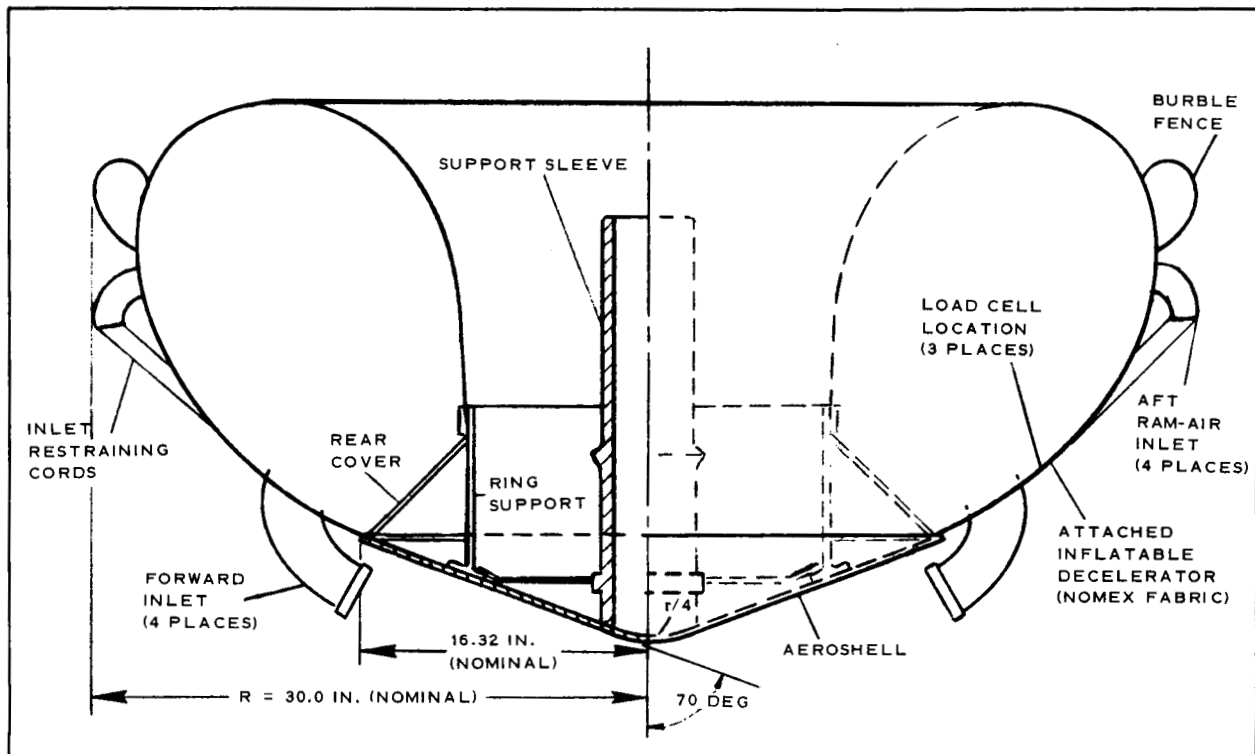


Figure 3. - Details of Model I Configuration

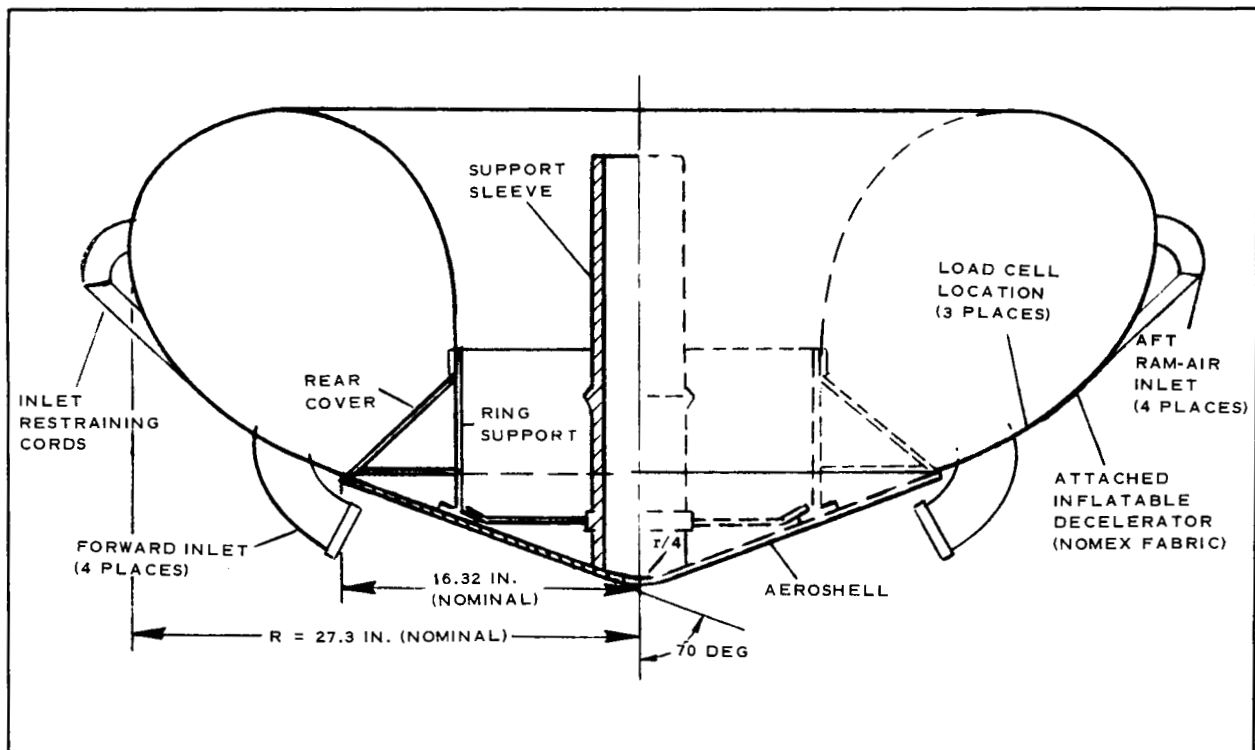


Figure 4. - Details of Model II Configuration

DESIGN CONDITIONS

The aerodynamic design conditions for the AID canopies are presented in Table II. The hard structure was designed to meet the requirements specified by Arnold Engineering Development Center (AEDC) in Reference 13.

TABLE II. - AID DESIGN CONDITIONS

Condition	Magnitude
Deployment Mach number, M	4.4
Deployment dynamic pressure, q (psf)	75.0
Maximum dynamic pressure, q (psf)	200.0

Shape Analysis

The AID canopy is basically a uniform-stress (isotensoid) structure (see Figure 5) whose shape is maintained by a balance of external aerodynamic loads and internal pressurization. The canopy shapes for the present models were derived using the isotensoid analysis described in References 2, 3, and 4. This analysis, computerized during a previous Goodyear Aerospace program (Reference 3) for LRC, uses a theoretical aerodynamic pressure distribution to calculate an initial shape which can then be used to obtain an experimental pressure distribution. This distribution is then inserted in the computerized analysis to obtain an "iterated" shape. This procedure can be repeated until the desired correlation is obtained.

Since numerous canopy shapes result from the isotensoid analysis the shape of the first-stage AID was obtained using an optimization procedure, described in Reference 14, to determine the decelerator shapes which combined the highest drag areas with the lowest canopy weights. The canopy shapes shown in Figures 3 and 4 were the result of this optimization study. Pertinent parameters (described in References 2, 3, and 4) for these shapes are presented in Table III. The pressure distributions used in deriving the shapes of models I and II are presented in Figures 6 and 7.

The internal canopy pressure was obtained from the empirical relation in Reference 3:

$$p/q_{\infty} = (p_i - p_b)/q_{\infty}$$

Experimental data taken from Reference 6 yielded a value of $p/q_{\infty} = 1.9$. This value was used to determine the stresses in the fabric and meridians as described in Appendix B.

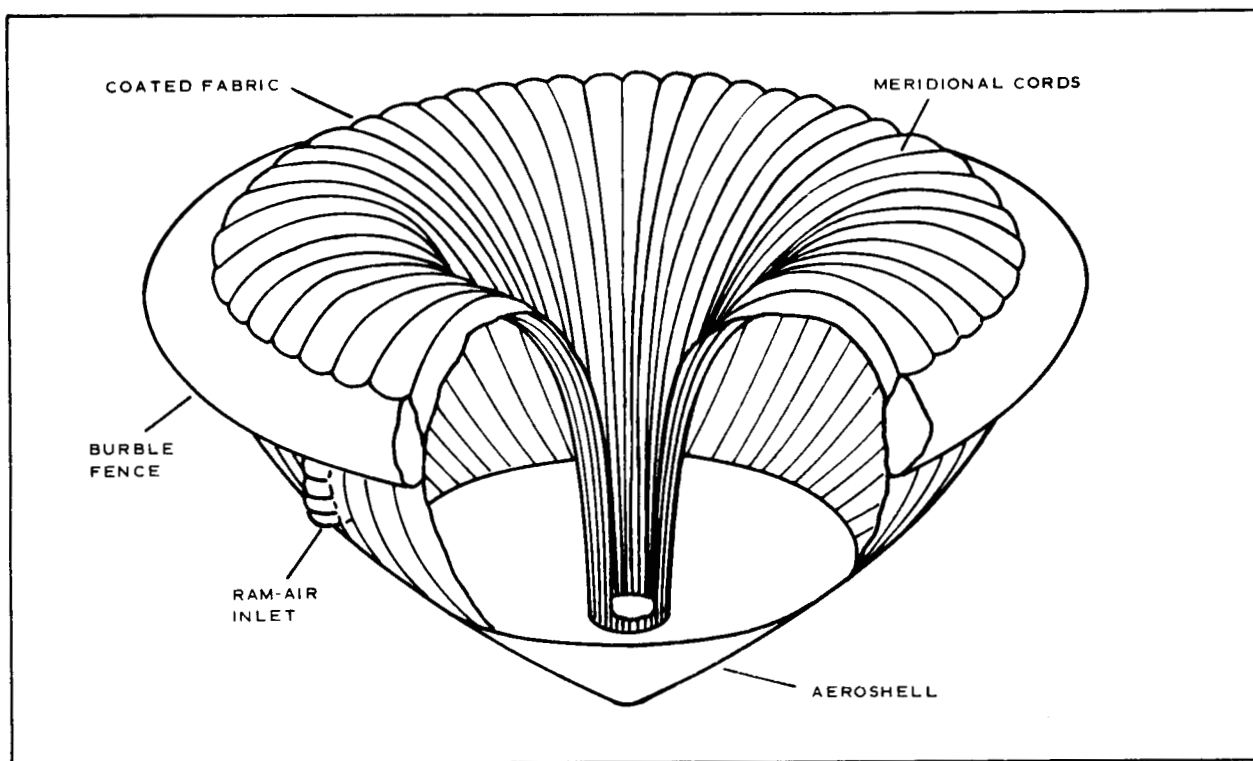


Figure 5 - Cutaway Drawing of an AID

TABLE III. - AID CANOPY PARAMETERS

Condition	Model I	Model II
Nondimensional meridian tape load, \bar{T}_r	0.38	0.38
Nondimensional fabric stress, \bar{f}_r	0.30	0.175
Ratio of circumferential fabric stress to meridional stresses, f_c/f_m	$0.8 \leq f_c/f_m \leq 1.8$	$0.8 \leq f_c/f_m \leq 1.8$
Nondimensional burble fence load, \bar{N}_B	0.0936	0.
Percent of burble fence load carried by front surface fabric, γ	0.1947	0.
Number of gores, n	60	60

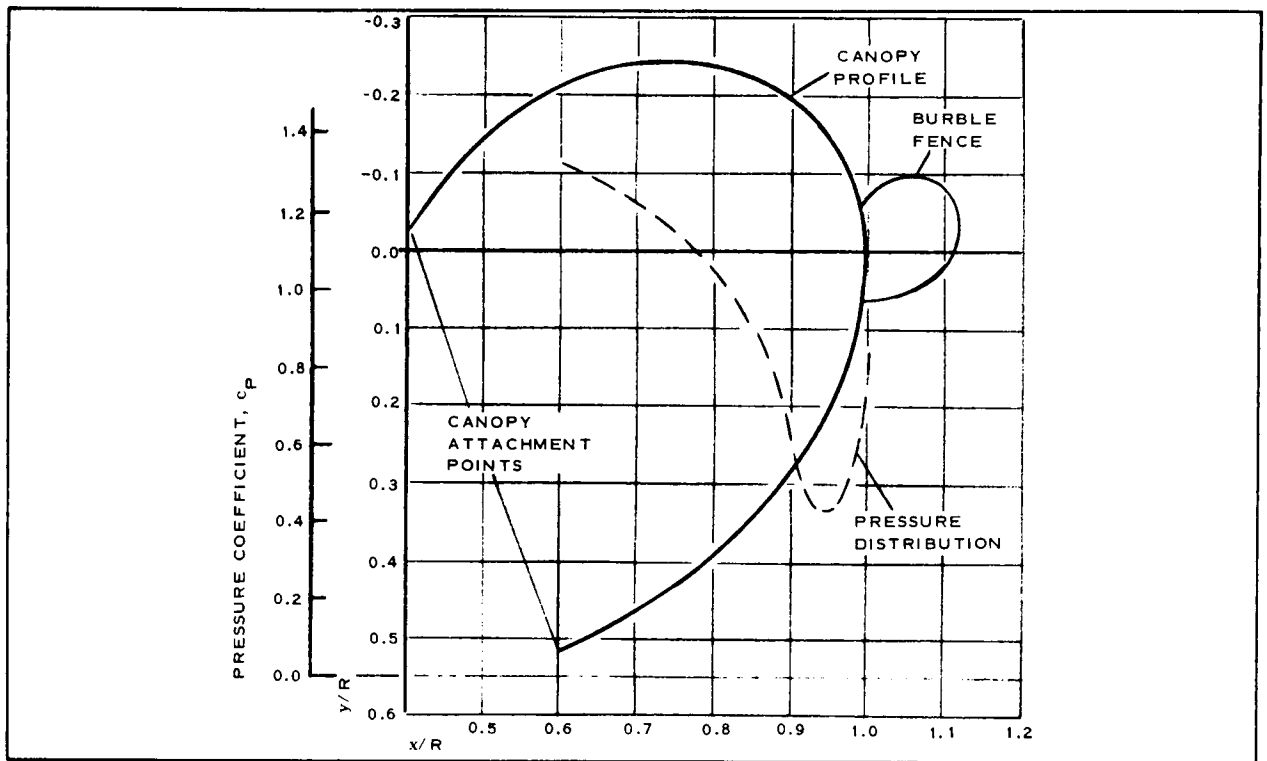


Figure 6. - Analytical Pressure Distribution for Model I

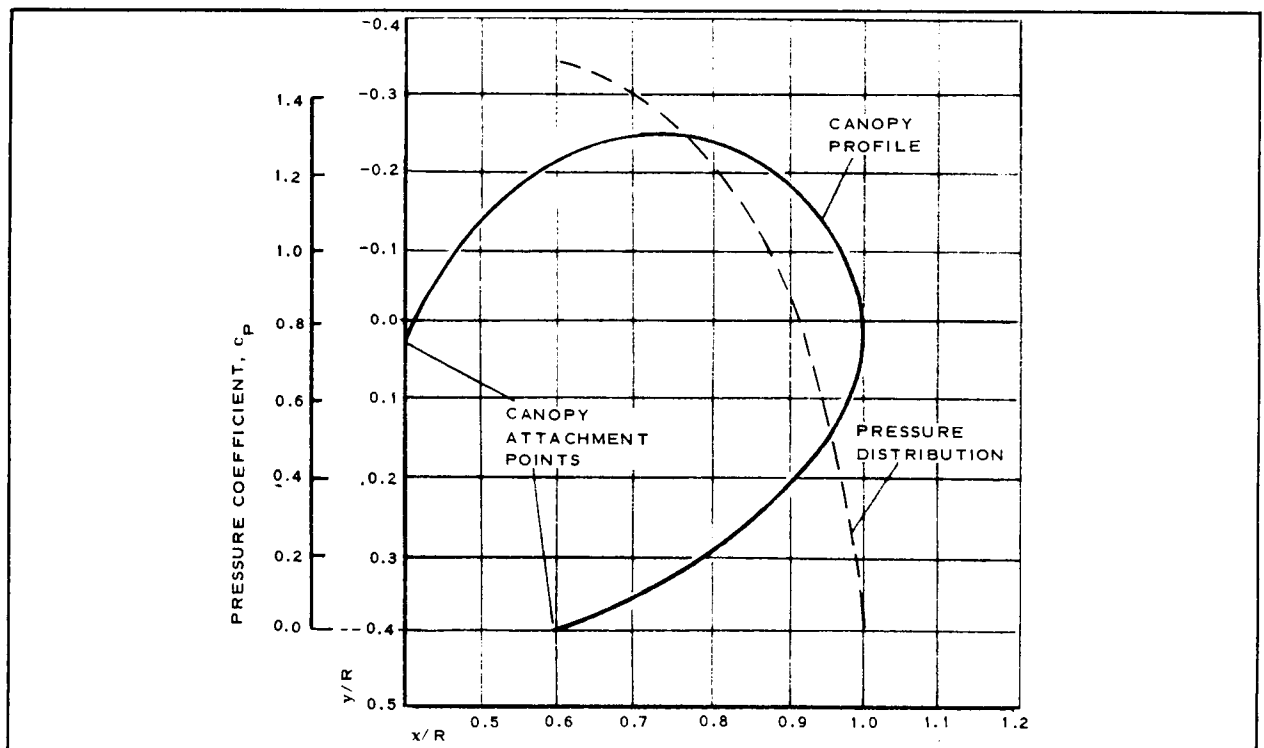


Figure 7. - Analytical Pressure Distribution for Model II

Canopy Gore Patterns

The nondimensional AID coordinates defining the canopy profile are one of the outputs of the isotenoid computer program. These coordinates have been tabulated for models I and II and are presented in Tables IV and V. Utilizing these coordinates in the analytical approach, established by the design analysis in Reference 3, it was determined that 60 gores were needed to maintain f_c/f_m within the limits set forth in Table III. The specific equations, derived in Reference 3, that define gore geometry are presented below. The numerical values of lobe geometry, radial growth due to unrestrained thread racking, and fabric stresses calculated from these equations are presented in Tables VI and VII.

$$\tan \beta = \frac{2\pi \left(\frac{x}{R}\right)}{n F} ;$$

$$\tan \gamma = \sqrt{\frac{\sin \beta \cos \beta}{\beta}} ;$$

$$\frac{r_g}{R} = \frac{\pi}{n \sin \beta} \left(\frac{x}{R}\right) ;$$

$$\frac{s_g}{R} = \left(\frac{r_g}{R}\right) \beta ;$$

$$\frac{d_g}{R} = \left(\frac{r_g}{R}\right) (1 - \cos \beta) ;$$

$$\epsilon_\phi = \sqrt{2} \sin \gamma - 1 ;$$

$$\epsilon_0 = \sqrt{2} \cos \gamma - 1 ;$$

$$f_b = F \frac{pR}{4} \left(\frac{\sin \beta}{\beta \sin^2 \gamma} \right) ; \text{ and}$$

$$\frac{f_c}{f_m} = \frac{1}{\tan^2 \gamma}$$

The gore patterns shown in Figures 8 and 9 each consist of three gores. Twenty of the patterns were used in constructing each model resulting in a total of 60 gores.

TABLE IV.- AID COORDINATES FOR MODEL I

x/R	y/R Front Surface	y/R Rear Surface
1.00000000E+00	0.	0.
9.99000000E-01	3.32819083E-02	-2.18055561E-02
9.75000000E-01	1.57445013E-01	-1.06822237E-01
9.50000000E-01	2.15344557E-01	-1.46923795E-01
9.25000000E-01	2.57259133E-01	-1.74868922E-01
9.00000000E-01	2.91124148E-01	-1.95961495E-01
8.75000000E-01	3.19948723E-01	-2.12278774E-01
8.50000000E-01	3.45388508E-01	-2.24885511E-01
8.25000000E-01	3.55328597E-01	-2.34409186E-01
8.00000000E-01	3.69548927E-01	-2.41240012E-01
7.75000000E-01	4.09314684E-01	-2.45535116E-01
7.50000000E-01	4.27876412E-01	-2.47760148E-01
7.25000000E-01	4.45423735E-01	-2.47712996E-01
7.00000000E-01	4.62103963E-01	-2.45550488E-01
6.75000000E-01	4.78934542E-01	-2.41275627E-01
6.50000000E-01	4.93311462E-01	-2.34552759E-01
6.25000000E-01	5.08013585E-01	-2.26202029E-01
6.00000000E-01	5.22207965E-01	-2.15192459E-01
5.75000000E-01	0.	-2.01628729E-01
5.50000000E-01	0.	-1.85228031E-01
5.25000000E-01	0.	-1.55579370E-01
5.00000000E-01	0.	-1.42065396E-01
4.75000000E-01	0.	-1.13725751E-01
4.50000000E-01	0.	-7.88773238E-02
4.25000000E-01	0.	-3.41413527E-02
4.00000000E-01	0.	-2.99577046E-02

TABLE V. - AID COORDINATES FOR MODEL II

x/R	y/R Front Surface	y/R Rear Surface
1.00000000E+00	0.	0.
9.99000000E-01	2.18208275E-02	-2.18055561E-02
9.75000000E-01	1.08690517E-01	-1.08322257E-01
9.50000000E-01	1.52395361E-01	-1.46923759E-01
9.25000000E-01	1.86225965E-01	-1.74868922E-01
9.00000000E-01	2.12351377E-01	-1.95961495E-01
8.75000000E-01	2.35798587E-01	-2.12278774E-01
8.50000000E-01	2.56617725E-01	-2.24885511E-01
8.25000000E-01	2.75437917E-01	-2.34409188E-01
8.00000000E-01	2.92672967E-01	-2.41240072E-01
7.75000000E-01	3.88612555E-01	-2.45535116E-01
7.50000000E-01	3.23459744E-01	-2.47750148E-01
7.25000000E-01	3.37406088E-01	-2.47712998E-01
7.00000000E-01	3.50548378E-01	-2.45550498E-01
6.75000000E-01	3.62998515E-01	-2.41275627E-01
6.50000000E-01	3.74839562E-01	-2.34852759E-01
6.25000000E-01	3.88101055E-01	-2.26202029E-01
6.00000000E-01	3.96961188E-01	-2.15192459E-01
5.75000000E-01	0.	-2.01528729E-01
5.50000000E-01	0.	-1.85228031E-01
5.25000000E-01	0.	-1.55579374E-01
5.00000000E-01	0.	-1.42068396E-01
4.75000000E-01	0.	-1.13725751E-01
4.50000000E-01	0.	-7.88773238E-01
4.25000000E-01	0.	-3.41413527E-01
4.00000000E-01	0.	2.99577046E-02

Table VI. - Model I Lobe Geometry, Radial Growth Due to Unrestrained Thread Racking, and Fabric Stresses

x/R	β		d_g/R	r_g/R	S_g/R	f_b lb/in.	γ		ϵ_ϕ	ϵ_θ	f_c/f_m
	deg	min					deg	min			
.60*	30	27	.02900	.06199	.0329	4.46	42	10	-.0507	.0482	1.219
.65	32	29	.02744	.06337	.0359	4.46	41	58	-.0543	.0515	1.232
.70	34	26	.02586	.06482	.0389	4.54	41	21	-.0670	.0627	1.294
.75	36	18	.02430	.06633	.0420	4.58	40	57	-.0733	.0681	1.326
.80	38	5	.02280	.06791	.0451	4.62	40	31	-.0712	.0751	1.370
.85	39	47	.02126	.06955	.0483	4.68	40	3	-.0900	.0825	1.415
.90	41	24	.01977	.07126	.0515	4.73	39	37	-.0982	.0894	1.457
.95	42	55	.01830	.07303	.0547	4.79	39	13	-.1060	.0956	1.504
1.00	44	25	.01680	.07481	.0579	4.84	38	46	-.1145	.1026	1.551
1.00	49	44	.02426	.06860	.0595	4.24	37	1	-.1486	.1291	1.762
.95	48	17	.02228	.06660	.0561	4.17	37	32	-.1386	.1213	1.695
.90	46	44	.02035	.06470	.0527	4.11	38	2	-.1289	.1130	1.632
.85	45	6	.01847	.06280	.0494	4.03	38	35	-.1182	.1053	1.571
.80	43	21	.01664	.06100	.0461	3.99	39	5	-.1086	.0975	1.519
.75	41	26	.01484	.05930	.0429	3.93	39	38	-.0980	.0890	1.457
.70	39	34	.01318	.05750	.0397	3.87	40	9	-.0883	.0810	1.404
.65	37	49	.01160	.05540	.0366	3.84	40	31	-.0827	.0734	1.369
.60	35	37	.01010	.05390	.0335	3.77	41	5	-.0721	.0643	1.315
.55	33	18	.00860	.05240	.0305	3.74	41	38	-.0620	.0553	1.267
.50	30	15	.00722	.05110	.0275	3.68	42	10	-.0521	.0466	1.217
.45	28	15	.00593	.04980	.0245	3.66	42	31	-.0458	.0407	1.188
.40	25	32	.00474	.04860	.0216	3.36	43	1	-.0367	.0324	1.150
.38	24	24	.00430	.04810	.0205	3.62	43	11	-.0337	.0296	1.137

* Indicates x/R value of forward attachment points for Models IA, IB, IC, and ID

Table VII. - Model II Lobe Geometry, Radial Growth Due to Unrestrained Thread Racking, and Fabric Stresses

x/R	β		d_g/R	r_g/R	S_g/R	f_b lb/in.	γ		ϵ_ϕ	ϵ_θ	f_c/f_m
	deg	min					deg	min			
.60*	35	37	.01010	.0539	.0335	3.77	41	5	-.0721	.0643	1.315
.65	37	49	.01160	.0554	.0366	3.84	40	31	-.0827	.0734	1.369
.70	39	34	.01318	.0575	.0397	3.87	40	9	-.0883	.0810	1.404
.75	41	26	.01484	.0593	.0429	3.93	39	38	-.0980	.0890	1.457
.80	43	21	.01664	.0610	.0461	3.99	39	5	-.1086	.0975	1.519
.85	45	6	.01847	.0628	.0494	4.03	38	35	-.1182	.1053	1.571
.90	46	44	.02035	.0647	.0527	4.11	38	2	-.1289	.1130	1.632
.95	48	17	.02228	.0666	.0561	4.17	37	32	-.1386	.1213	1.695
1.00	49	44	.02426	.0686	.0595	4.24	37	1	-.1486	.1291	1.762
.95	48	17	.02228	.0666	.0561	4.17	37	32	-.1386	.1213	1.695
.90	46	44	.02035	.0647	.0527	4.11	38	2	-.1289	.1130	1.632
.85	45	6	.01847	.0628	.0494	4.03	38	35	-.1182	.1053	1.571
.80	43	21	.01664	.0610	.0461	3.99	39	5	-.1086	.0975	1.519
.75	41	26	.01484	.0593	.0429	3.93	39	38	-.0980	.0890	1.457
.70	39	34	.01318	.0575	.0397	3.87	40	9	-.0883	.0810	1.404
.65	37	49	.01160	.0554	.0366	3.84	40	31	-.0827	.0734	1.369
.60	35	37	.01010	.0539	.0335	3.77	41	5	-.0721	.0643	1.315
.55	33	18	.00860	.0524	.0305	3.74	41	38	-.0620	.0553	1.267
.50	30	15	.00722	.0511	.0275	3.68	42	10	-.0521	.0466	1.217
.45	28	15	.00593	.0498	.0245	3.66	42	31	-.0458	.0407	1.188
.40	25	32	.00474	.0486	.0216	3.63	43	1	-.0367	.0324	1.150
.38	24	24	.00430	.0481	.0205	3.62	43	11	-.0337	.0296	1.137

* Indicates x/R value of forward attachment point for models IIA and IIB

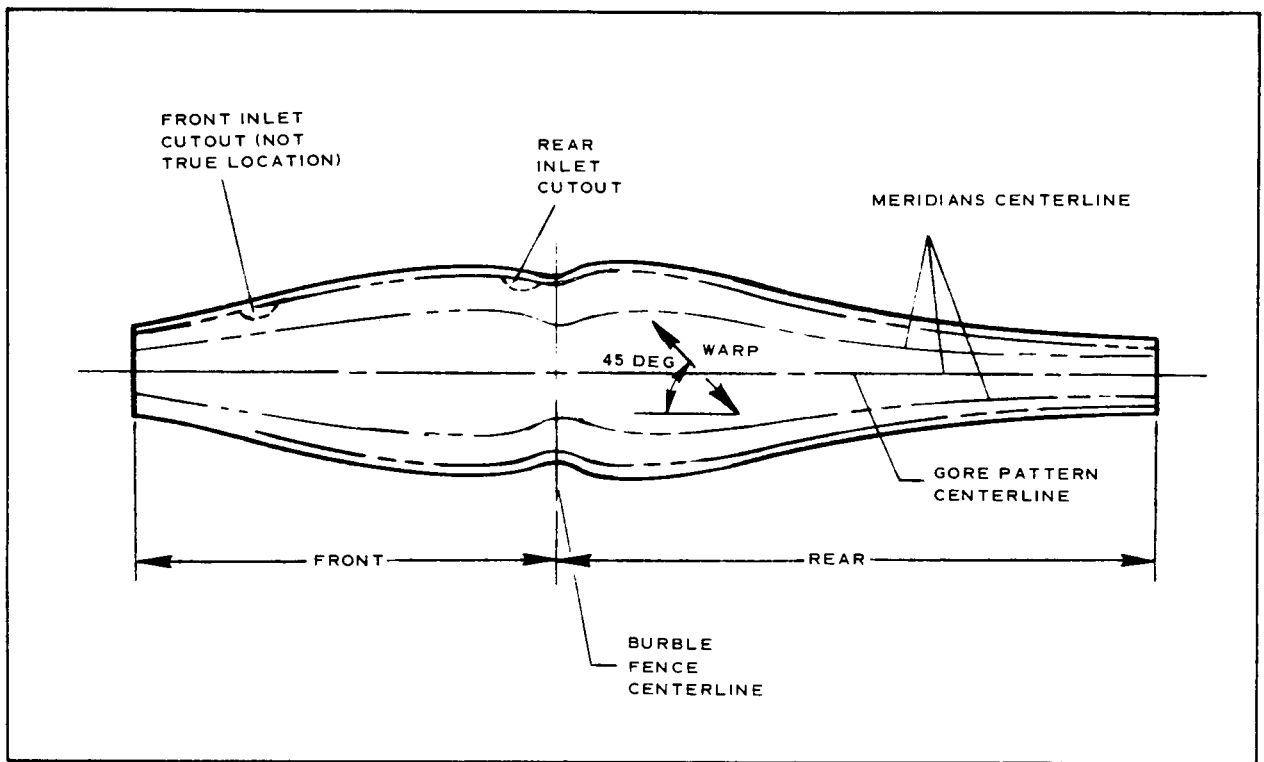


Figure 8. - Model I Gore Pattern

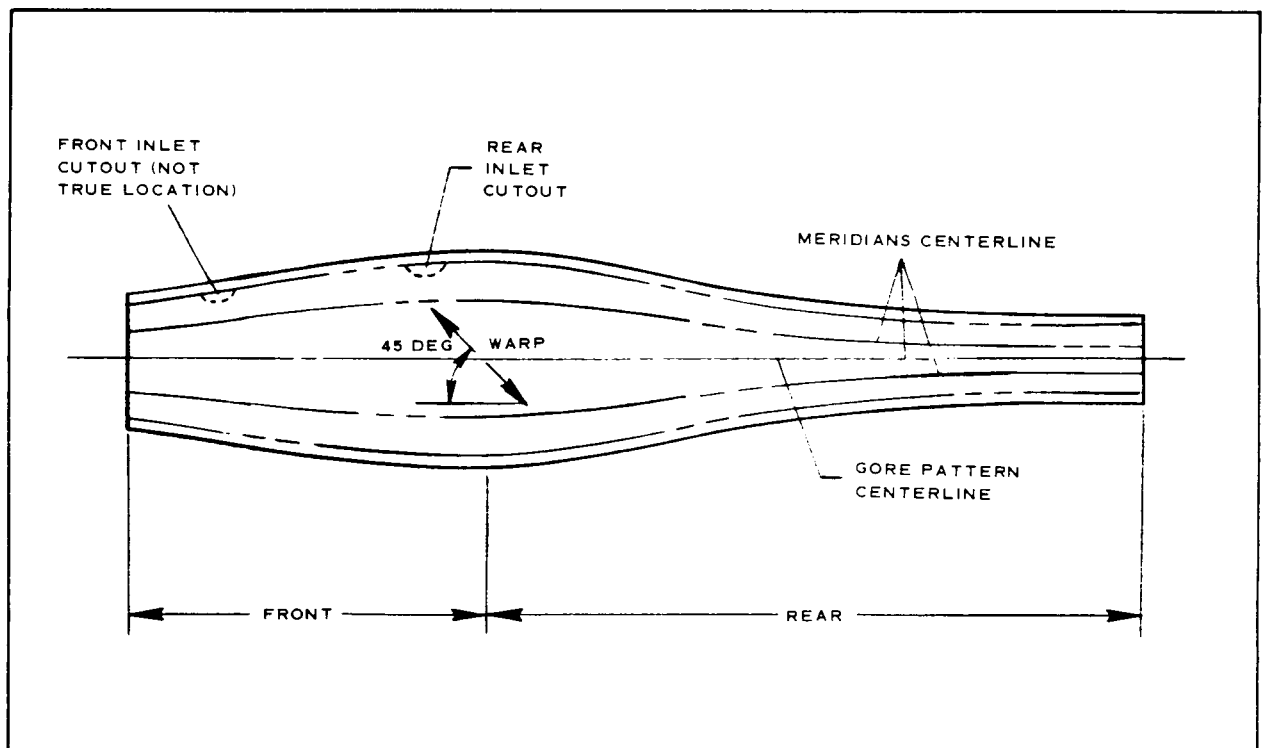


Figure 9. - Model II Gore Pattern

Inlet Sizing

One of the present program's objectives was to investigate the effects of inlet size on canopy deployment and inflation. Wind-tunnel tests (Reference 6) conducted previously used AIDs with aft inlets larger in area than the forward inlets. In this investigation, it was of interest to determine the effects of aft inlets equal to and smaller than the area of the forward inlets.

The four forward inlets were selected as 2.5 in. in diameter based upon the satisfactory performance of the same size inlets in the wind-tunnel tests described in Reference 6. Accordingly, the four aft inlets were 2.5 in. in diameter and 1.8 in. in diameter, the latter being the same size as the inlets on the models described in Reference 9. The combination of the inlets on the models is presented in Table VIII.

TABLE VIII. - AID INLET SIZES

Model	Forward Inlet Diameter (in.)	Aft Inlet Diameter (in.)
IA	2.5	2.5
IB	2.5	1.8
IC	2.5	2.5
ID	2.5	1.8
IIA	2.5	2.5
IIB	2.5	2.5

An inflation analysis computer program was developed by Goodyear Aerospace under this investigation which predicts AID model inflation times. This program, described in Reference 9, verified that both inlet size combinations would inflate the current models within the 1.0-sec design goal.

SYSTEM DESIGN

Forward Inlets

The forward canopy inlets incorporate torsion springs to deploy and to hold the inlets in the air flow. The springs, similar to those used on the models of Reference 6, were selected on a basis of their mechanical simplicity and demonstrated reliability.

The spring design is basically that of a torsion spring. The spring rotates about an aluminum shaft which is attached to the outer ring by two clamps. The free ends of the spring are fastened to the outer ring by an aluminum clamping block (see Figure 10). The spring has a preload torque of $20.6 \pm .05$ in.-lb at an angle of 70 deg (Figure 11) and a maximum torque of 40.7 ± 1 in.-lb at an angle of 275 deg when in the packed condition.

The construction of the fabric inlets was identical to the techniques used on the inlets described in References 3 and 9. The mouth of the inlet incorporates a wire loop which serves to prevent the inlet from collapsing during inflation and to which the ring section of the torsion spring is attached (see Figure 12).

Aft Inlets

The aft inlets are identical in construction to those on the models of Reference 9. Two different size inlets were fabricated as presented in Table VIII.

The forward and aft inlets were placed at 45 deg relative to each other in order to prevent flow interference and to provide symmetry (see Figure 13). No canopy meridians were cut as a result of this placement.

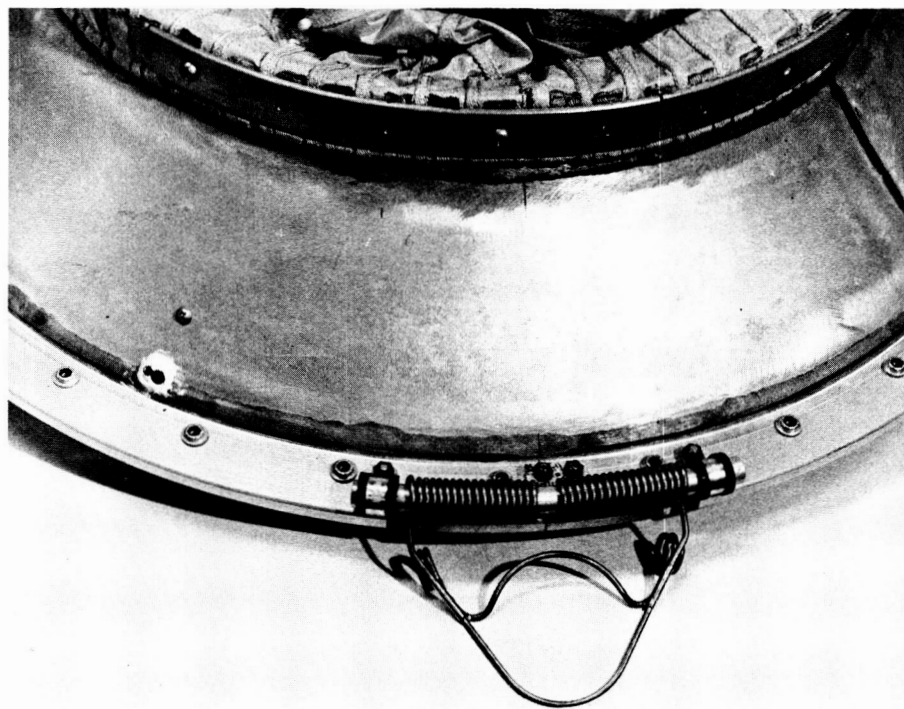


Figure 10. - Forward Inlet Spring Attached to Hard Structure

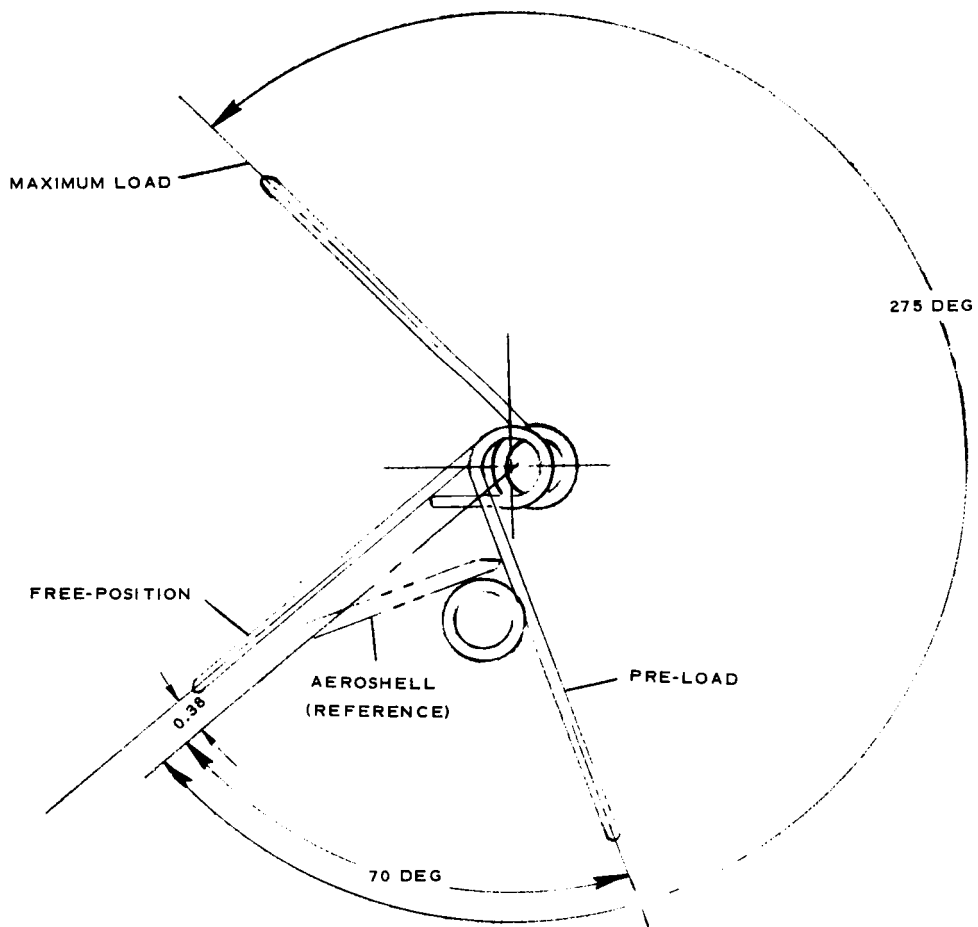


Figure 11. - Forward Inlet Spring Positions

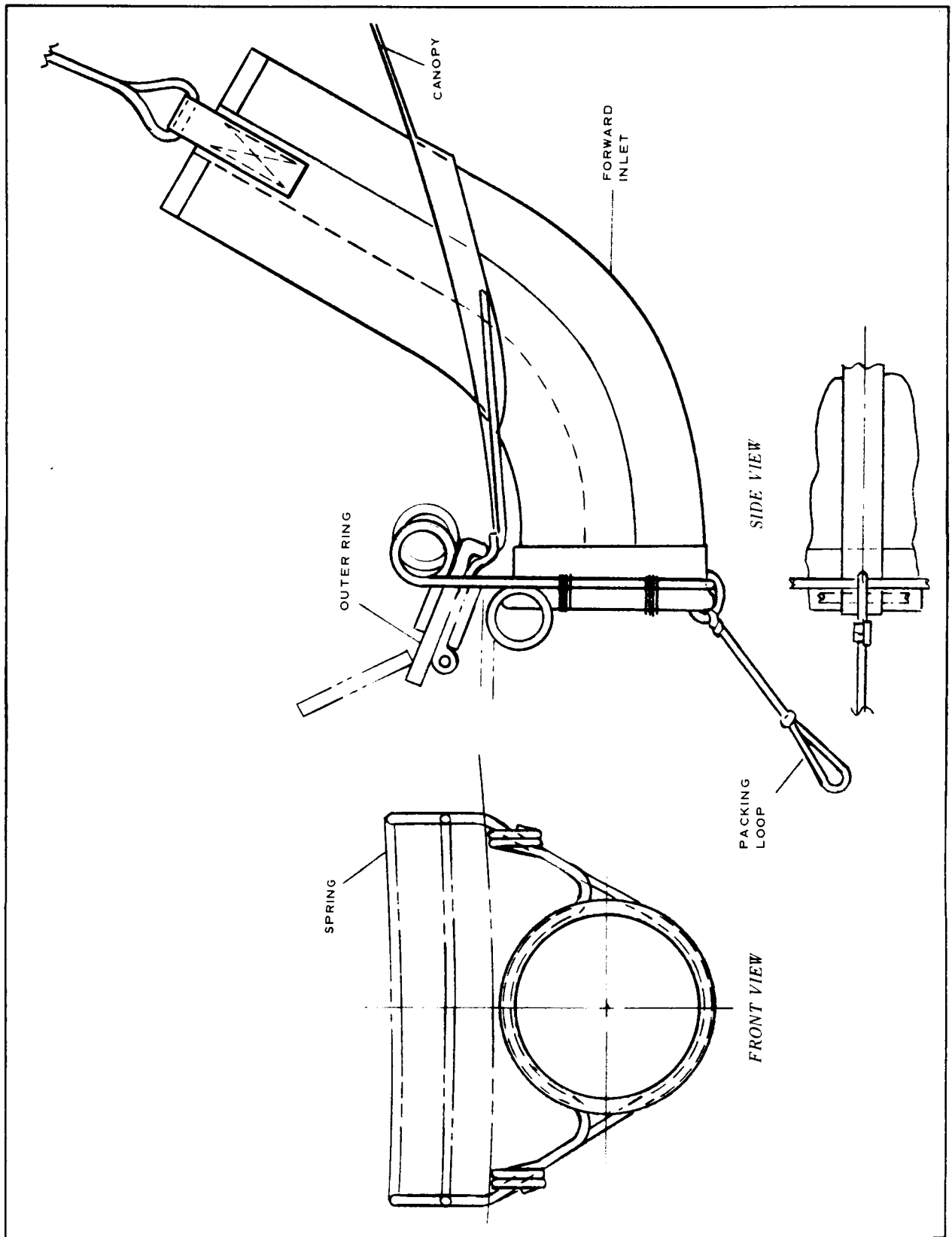


Figure 12. - Forward Inlet Sketch

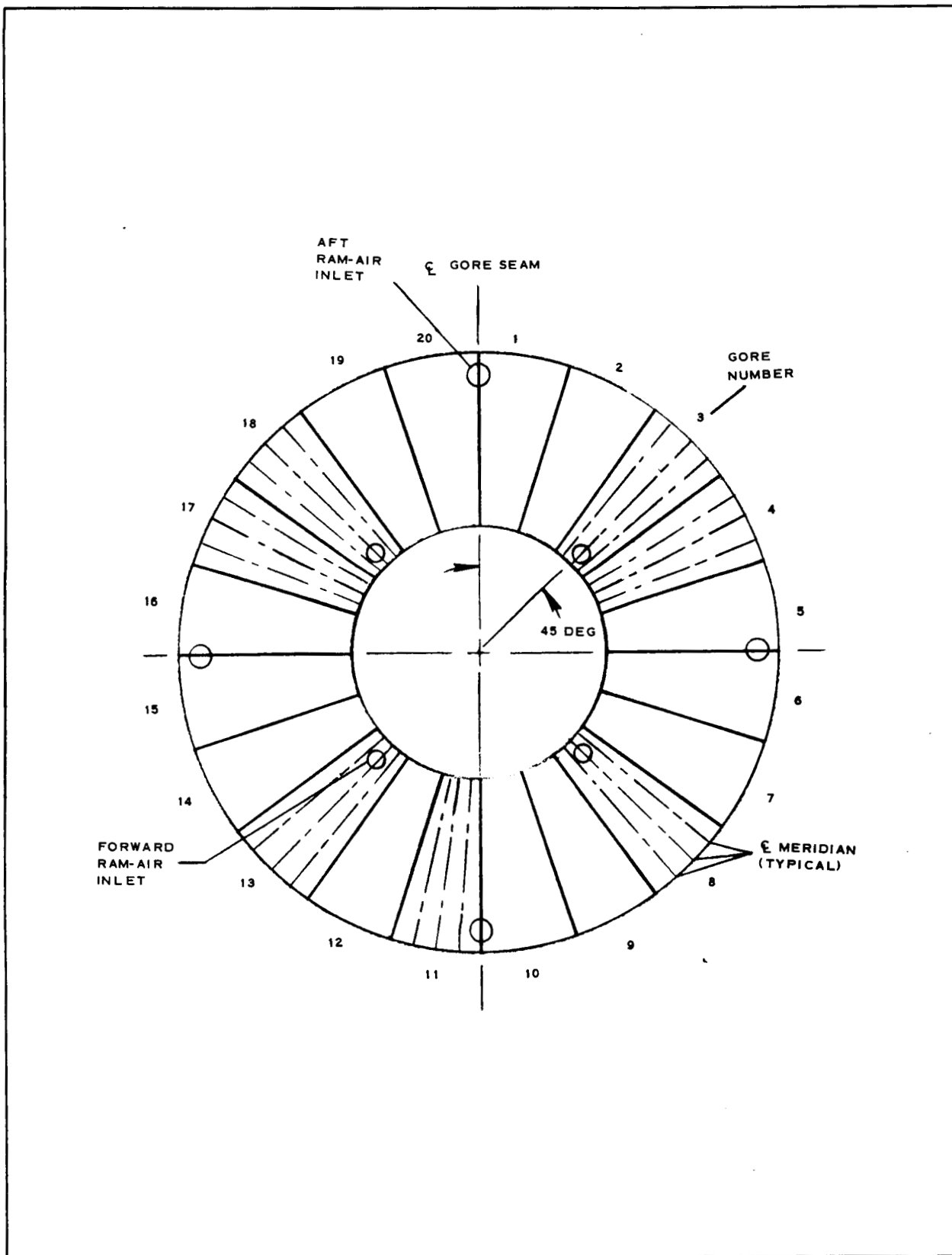


Figure 13. - Relative Angular Displacement of Inlets (Looking Downstream)

Canopy Attachment Scheme

Figure 14 shows the method of attaching the canopy to the hard structure. The aft canopy clamping band is held to the ring support by six clamping sectors (see Figure 10). The forward canopy clamping band is attached to the outer ring by a large clamping ring. Fabric spacers made of webbing similar in thickness to the meridional tapes were sewn in between each meridian at the attachment to provide a better clamping surface. A layer of epoxy was used in the interface between the fabric and metal structure under the clamping rings and in all the fabric-metal joints to prevent air leakage.

Canopy Storage and Release

It is very important that the canopy be packaged in a manner which: (1) eliminates frictional heating due to excess rubbing of the fabric and (2) provides for the erection of the inlets in the airstream for immediate inflation and ram-air pressurization. Several methods of folding and restraining the AIDs were investigated to ensure that the best packaging method would be selected.

Details of canopy folding pattern are shown in Figure 15. The outer fold of the AID was brought straight back to the top edge of the inner ring. A canopy stowage loop was placed on each meridian through which a restraining cord was passed to hold the canopy tightly against the rear surface. The cord was also passed through six pyrotechnic cutters spaced equidistantly around the top inner surface of the ring support (see Figure 16). Activation of the cutters will sever the cord in six places allowing it to be pulled through the loops as the AID inflates. The cord was terminated in a tuck-splice to allow the end to pass through the loops without interference.

The forward inlets were secured in a similar manner. A cord was passed through the loop attached to each inlet, through two pyrotechnic cutters, and terminated in a tuck splice (see Figure 16). In their stowed position, the inlets are held out of the air flow against the canopy. Release of the spring-mechanisms will occur when the cutters are fired.

MODEL INSTRUMENTATION

Each model was instrumented with one pressure transducer for measuring internal canopy pressure-time history; and three load cells for measuring meridional tape load-time history.

One pressure transducer, having a ± 5.0 psid range, was mounted on the back surface of each model's rear cover so as not to interfere with the packing of the canopy against the rear cover. Two rubber

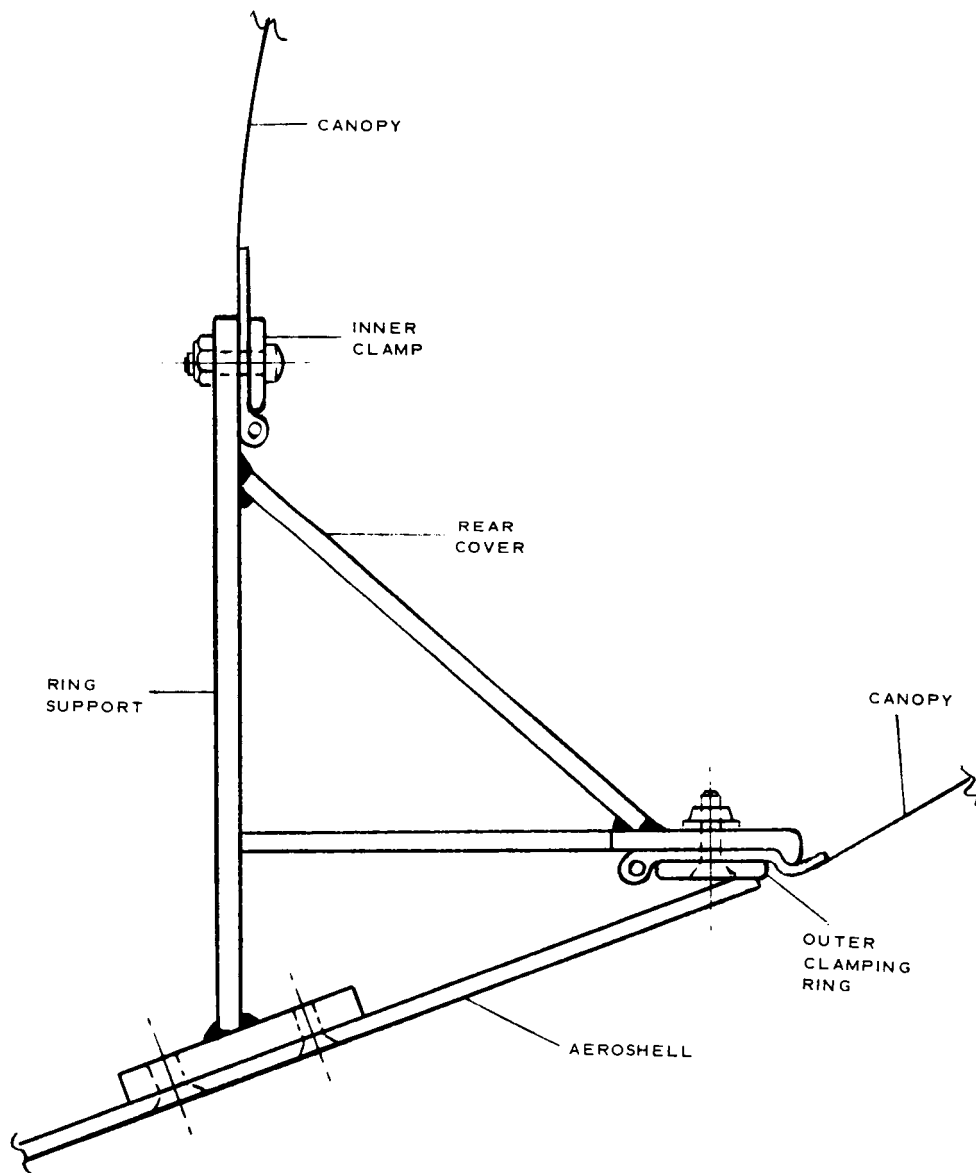


Figure 14. - Canopy Attachment Scheme

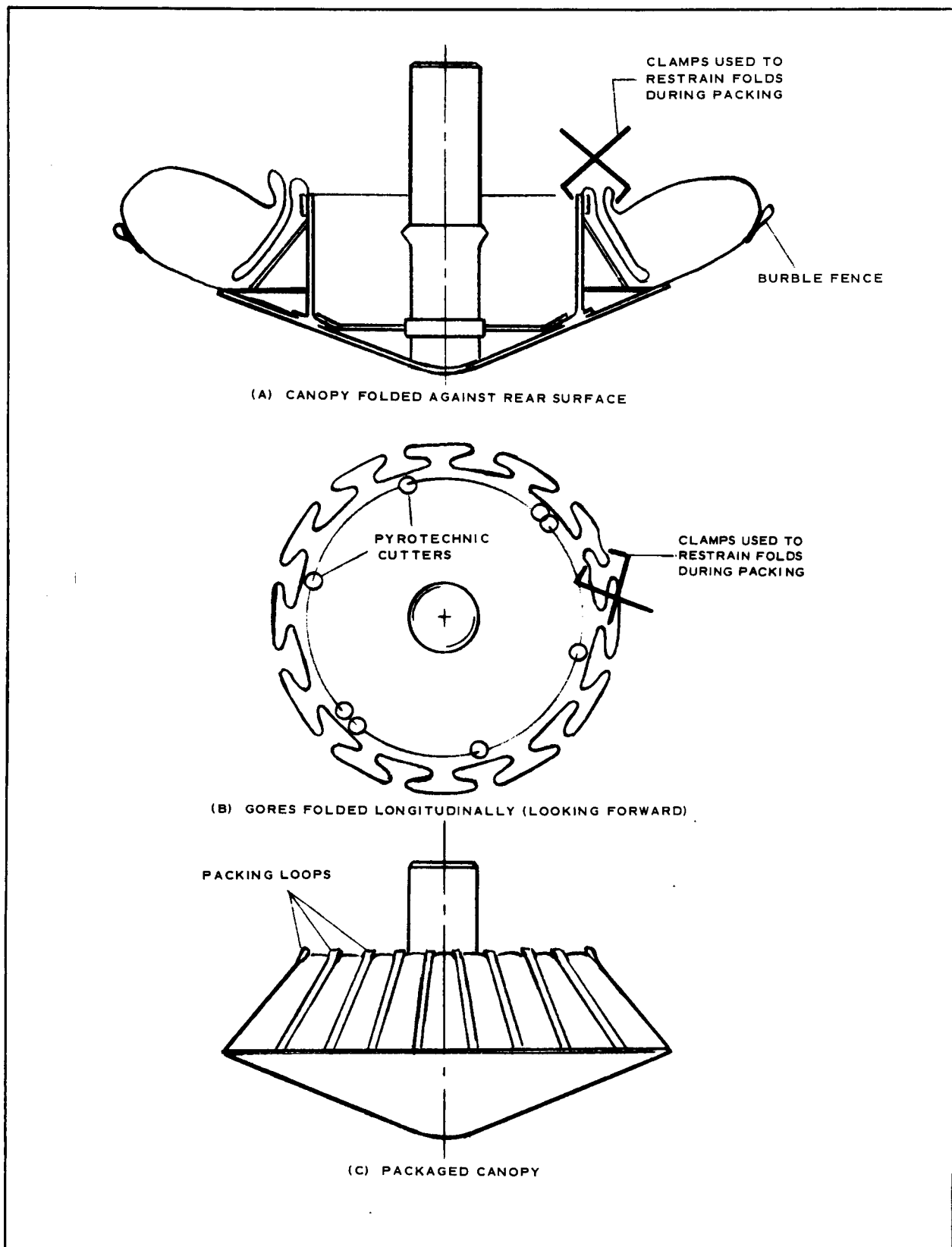


Figure 15. - Canopy Stowage and Release Scheme



Figure 16. - AID Model in Packaged Configuration

tubes extended through an opening in the rear cover into the internal canopy for sensing pressure (see Figure 10). One tube was attached to the pressure transducer; the other tube is for use in measuring final canopy pressure.

The load cells, each capable of measuring up to 180 pounds, were installed on each of three meridional tapes symmetrically on the front surface at $x/R = 0.70$ as shown in Figure 17. Exact load cell locations and load cell numbers for each model are shown in Figure 18.

PIVOTAL BALANCE ADAPTER

A pivotal balance adapter support sleeve (see Figure 19) was designed and fabricated by GAC for use in wind-tunnel testing the current models. This adapter, which permits the models' freedom in pitch and yaw, was designed to mate with the AEDC sting system designated S-5.53M-123-9.12M (Reference 15).

The adapter consists of four major components: an aeroshell attachment arm, a spherical bearing, a locking pin and a hydraulic cylinder. In operation, the locking pin is seated in the bearing preventing the model from moving during tunnel start and shutdown. During the test, the pin will be withdrawn by the hydraulic cylinder allowing the model freedom to pivot. Rotational motion is limited by two radial pins.

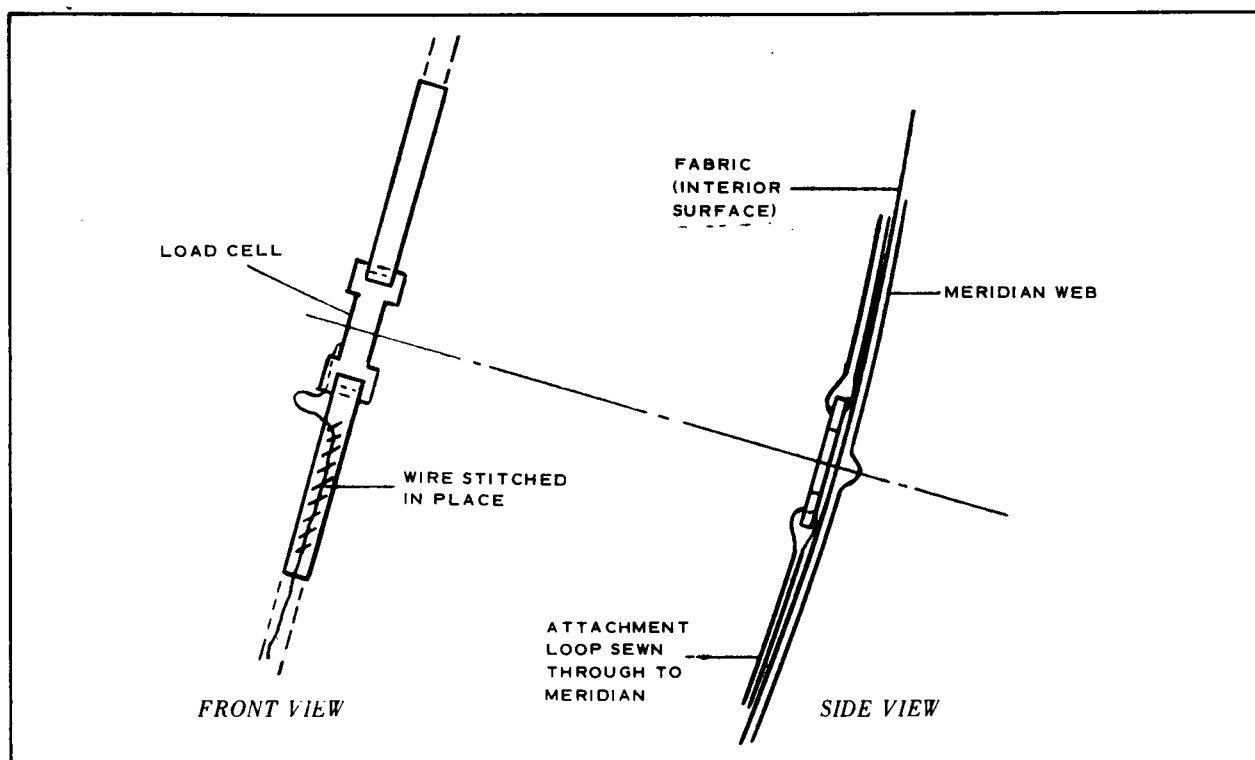


Figure 17.-Load Cell Attachment to Meridian

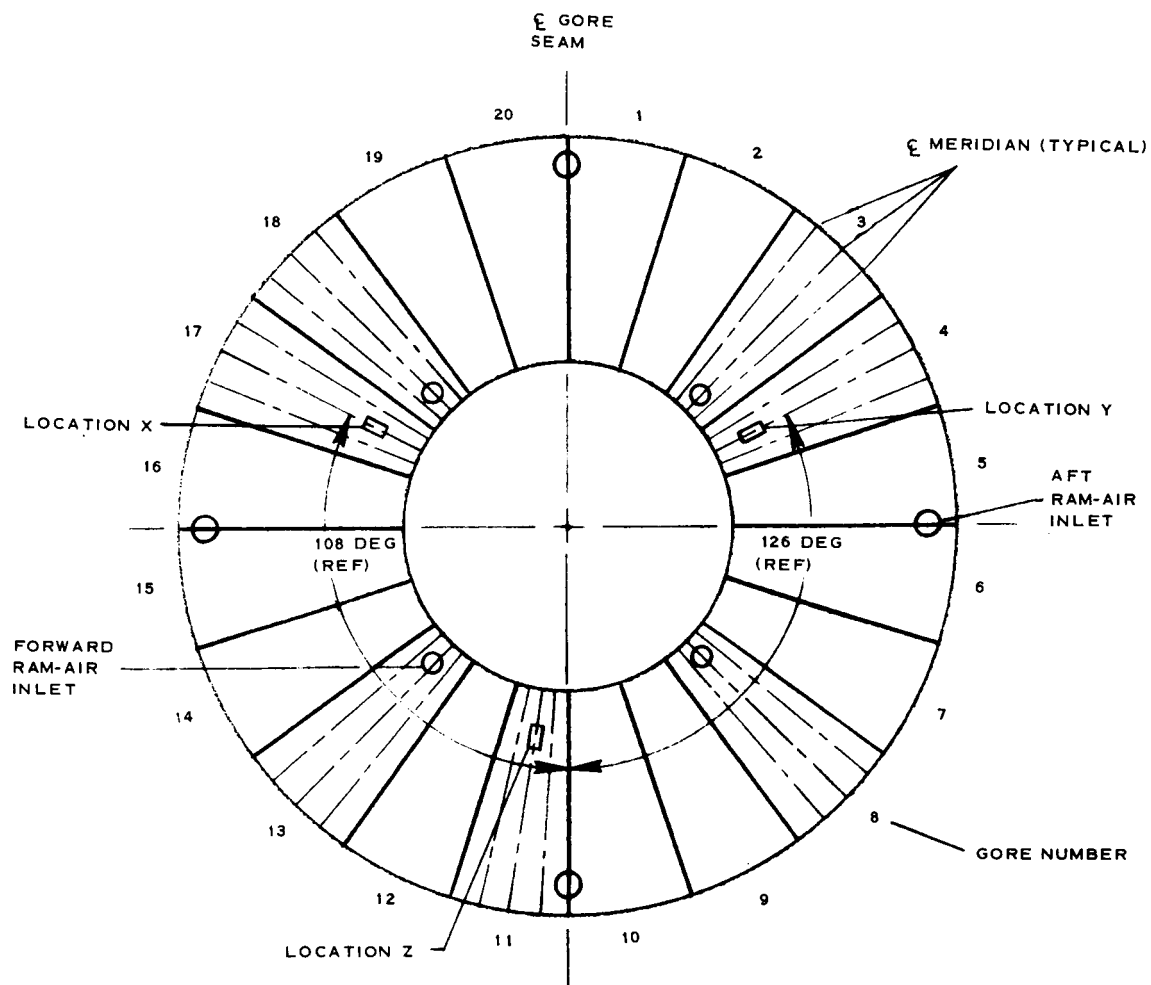
The adapter will permit angular movement in pitch and yaw up to ± 20 deg and in rotation up to ± 15 deg. The pivot bearing has a rated radial load of 123,000 lb and a rated thrust load of 30,875 lb. The hydraulic cylinder is rated at 1500 psi. The time required for the locking pin to release the model is approximately 1 sec at a pressure of 500 psi.

The pivotal adapter was tested after fabrication to demonstrate its ability to withstand aerodynamic loads expected in the wind tunnel. The setup for this test is shown in Figure 20. The tests showed that displacement caused by induced moments were within acceptable limits. A weight analysis summary which presents the center of gravity locations for Model I and II configurations and component weights is found in Appendix C.

MATERIAL SELECTION

Hard Structure

The aeroshells were spun-form from aluminum alloy sheets into final shape. A rigid, close-fitting, low-carbon steel tube serves as the transitional support sleeve between the sting-mounted internal balance and the aeroshells on models IA, IB, and IIA. Models IC,



MODEL NO.	POSITION	SERIAL NUMBER
IA	X	1
	Y	2
	Z	3
IB	X	7
	Y	8
	Z	9
IC	X	4
	Y	5
	Z	6

MODEL NO.	POSITION	SERIAL NUMBER
ID	X	10
	Y	12
	Z	13
IIA	X	15
	Y	16
	Z	14
IIB	X	17
	Y	18
	Z	19

Figure 18. - Serial Numbers and Locations of Load Cells for Each Model

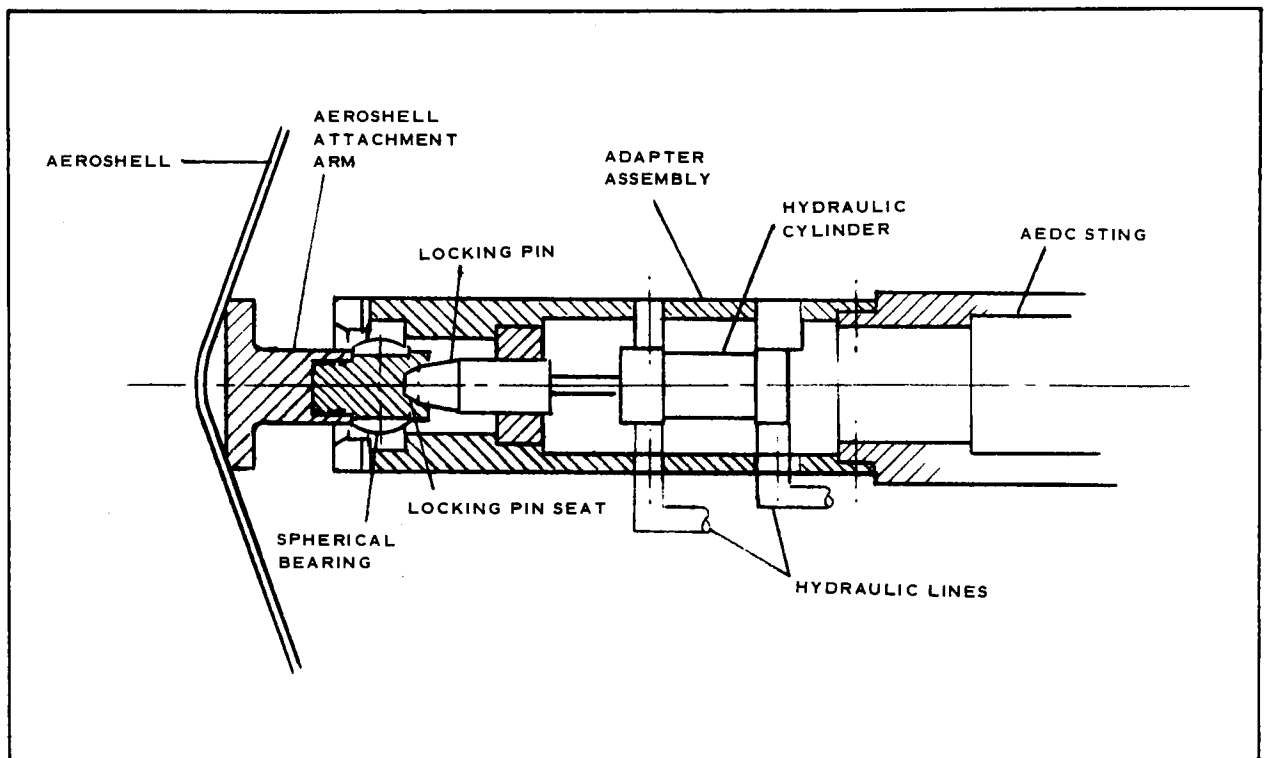


Figure 19. - Sketch of Pivotal Adapter

ID, and IIB utilize the pivotal adapter, described above, as the transitional support. A hardened steel mounting pin is the load-carrying member between each support sleeve and the AEDC balance.

The AID was secured to the hard structure by clamping the canopy end bands (see Figure 14). Attachment to the outer ring was achieved by a 6061-T6 aluminum alloy clamping ring; inner attachment to the ring support was accomplished by six 6061-T6 aluminum alloy clamping sectors. The remainder of the hard structure was fabricated from 6061 aluminum alloy and welded in accordance with Reference 13 requirements (see Drawing 3063000-003, Appendix A).

Fabric

All six models were fabricated from Nomex cloth. The cloth was calendered* and coated to reduce its permeability to a level such that the ram-air pressurization through the inlets would maintain the design shape and internal pressure.

*Calendering of the cloth is a mechanical process for reducing the fabric permeability by passing a heated mandrel under pressure over the cloth. The cloth is restrained at its perimeter to reduce shrinkage.

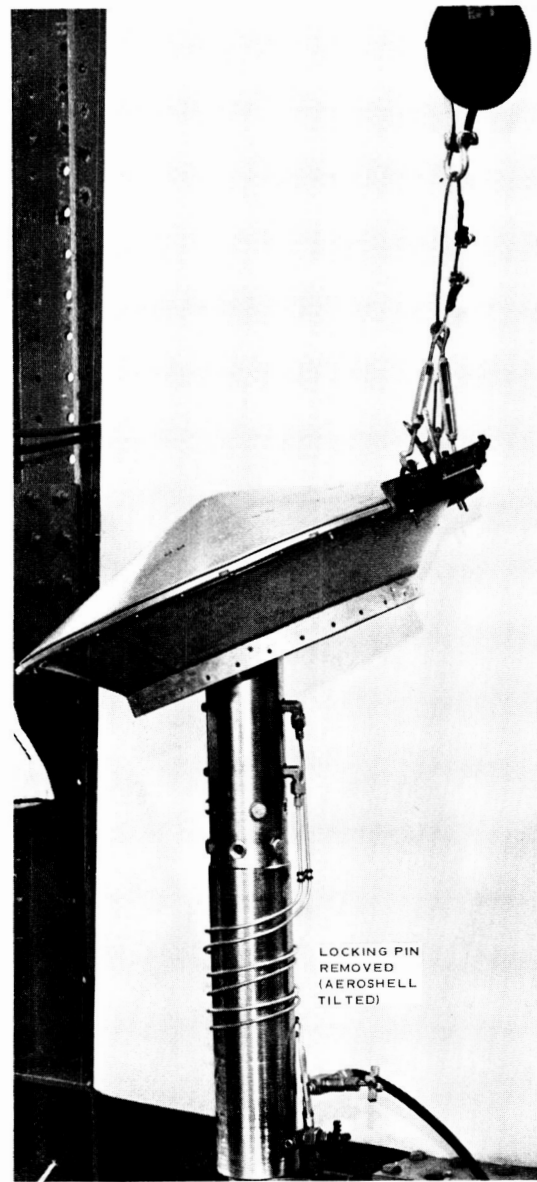
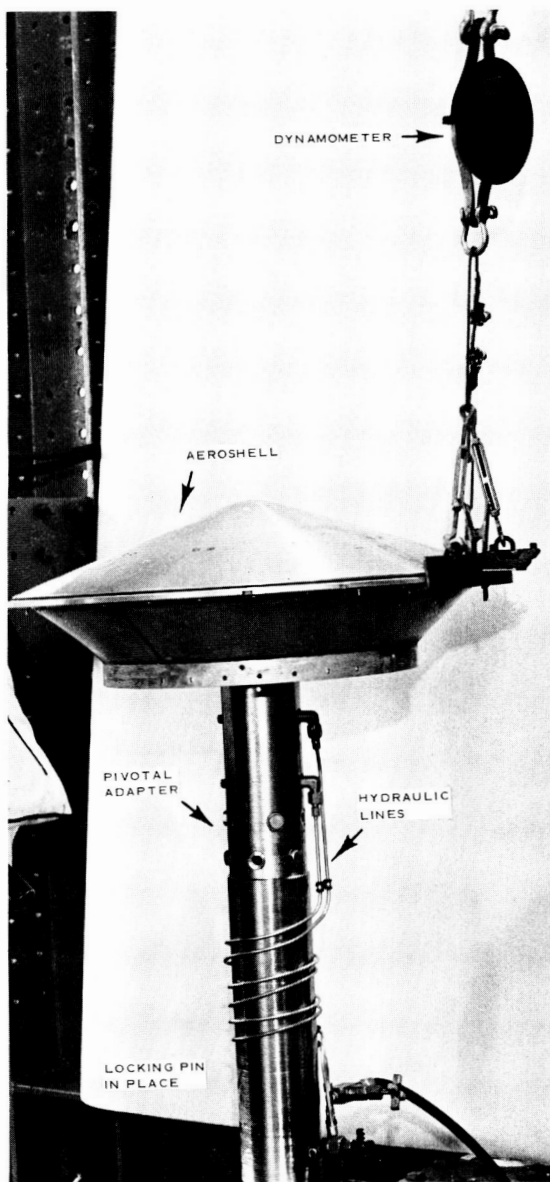


Figure 20. - Test Setup of Static Test of Pivotal Adapter

The Nomex fabric was coated with 0.4 oz/sq yd of the same Viton fluorelastomer which had been successfully employed in the model designs of References 3, 6, and 9. The coating was applied by machine, predried at 150 deg, and final cured at 325 deg F.

The meridional tapes are similar to MIL-T-5038 Type V tape but were specially woven of Nomex instead of nylon. To simulate the relative meridian size better, the 500-lb tape was folded to 1/4 in. wide for attachment to the fabric. The gore and the burble fence seams used a simple lap seam, 5/8 in. wide, and two rows of Federal Specification 751 Type 301 lockstitching and one row of single-throw Type 304 zig-zag stitching. The zig-zag stitch was used to secure the edge of the fabric that is exposed to the airstream. To reinforce the gore around the inlet, a Goodyear Aerospace-developed, 300-lb braided Nomex cord was sewn in place. Actual loads for both the fabric and meridional tapes are calculated in Appendix B.

DEVELOPMENT TESTS

General

Development tests conducted include: (1) tensile tests of both the uncoated and uncalendered Nomex and the calendered and coated Nomex fabric, (2) permeability tests of the calendered and coated Nomex fabric, and (3) a rapid deployment and inflation test of one of the completed AID models.

Tensile Tests of Nomex Fabric

Variations in the tensile strength characteristics of textile materials woven to the same specification can occur among different lots. To account for these variations, it was necessary to conduct tensile strength tests to determine the exact strength characteristics of the lot used. Tensile tests were conducted on 1-in. ravelled strips of both the uncoated and uncalendered Nomex fabric (HT-189) and the coated and calendered Nomex fabric (GX601V0262) in accordance with Federal Specification CCC-T-191b on a tensile testing machine. A summary of these tests is presented in Table IX. Strength tests were not conducted on the Nomex meridional tapes or the various thread types used in the fabrication of the canopies. These materials were taken from the same lot as the materials used in the fabrication of earlier models, the strength of which is documented in References 3 and 10. The gore seams, burble fence seams, and inlets seams were identical to those used on the models in References 3 and 6; and as a result, strength tests were not repeated during this program. The structural integrity of the load cell attachment to the meridians, the forward inlet, and the forward attachment was established by the tensile tests of Reference 9.

TABLE IX. - TENSILE STRENGTH TEST
RESULTS OF CANOPY FABRIC

Specimen	HT-189 Fabric Ultimate Load (lb/in.)	GX601V0262 Fabric Ultimate Load (lb/in.)
Warp Direction		
1	101.0	93.0
2	99.0	95.0
3	105.0	101.0
4	102.0	97.0
5	101.0	99.0
Average	101.6	97.0
Fill Direction		
1	120.0	115.0
2	115.0	106.0
3	118.0	110.0
4	117.0	111.0
5	119.0	113.0
Average	117.8	111.0

Fabric Permeability Tests

To obtain the high pressure recovery needed to produce the design shape and design drag coefficient, the Nomex was calendered and coated to reduce its permeability level. The results of this operation provided a permeability of approximately 0.5 cu ft/sq ft-min at 1/2 in. of water. Experience has shown that sewing operations and normal handling will tend to increase the permeability level slightly up to that required of 1.0 cu ft/sq ft-min at 1/2 in. of water.

Deployment and Inflation Test

To demonstrate the adequacy of the packaging, deployment, and inflation characteristics of the models, a deployment and inflation test was conducted in an environmental chamber. Model IC successfully deployed and inflated at the following conditions: 20 psfa and approximately 170 deg F. These conditions were established by deployment and inflation tests in Reference 3.

Inflation was initiated by rapid vaporization of a water-alcohol solution contained in a reservoir within the packaged canopy. A pressure transducer mounted internally and load cells attached to the canopy provided measurements of the differential pressure and the loads imposed on the meridians during deployment.

The inflation test setup, Figure 21, describes the sequence of events. A shape controlling spoked guide shown in Figure 21 serves to cradle the AID when inflated preventing the canopy from inflating in a distorted shape due to the absence of aerodynamic loads (Reference 3).

The differential pressure-time history of the AID during its deployment and inflation is shown in Figure 22. Full inflation of the canopy occurred in 0.36 sec. Load cell force-history for the three load cells are shown in Figure 23. The peak loads occurred just prior to inflation. Figure 24 is a picture of the AID model at full inflation. A review of the film coverage of the test indicated that the packaging and deployment scheme was suitable for use in the wind tunnel.

CONCLUSIONS

Six first stage attached inflatable decelerator models have been designed and fabricated for supersonic wind-tunnel evaluation. The models incorporate spring-actuated forward inlets for initial deployment and aft inlets for full inflation and final pressurization. The model I configurations differ from the model II configurations by the presence of a 10-percent burble fence and the resultant geometry change. The following conclusions can be drawn: (1) a canopy which simulated a first-stage AID both in shape and attachment locations was designed and fabricated; (2) the workability of the models' packaging and restraining system, and successful AID deployment were demonstrated during a rapid inflation test.

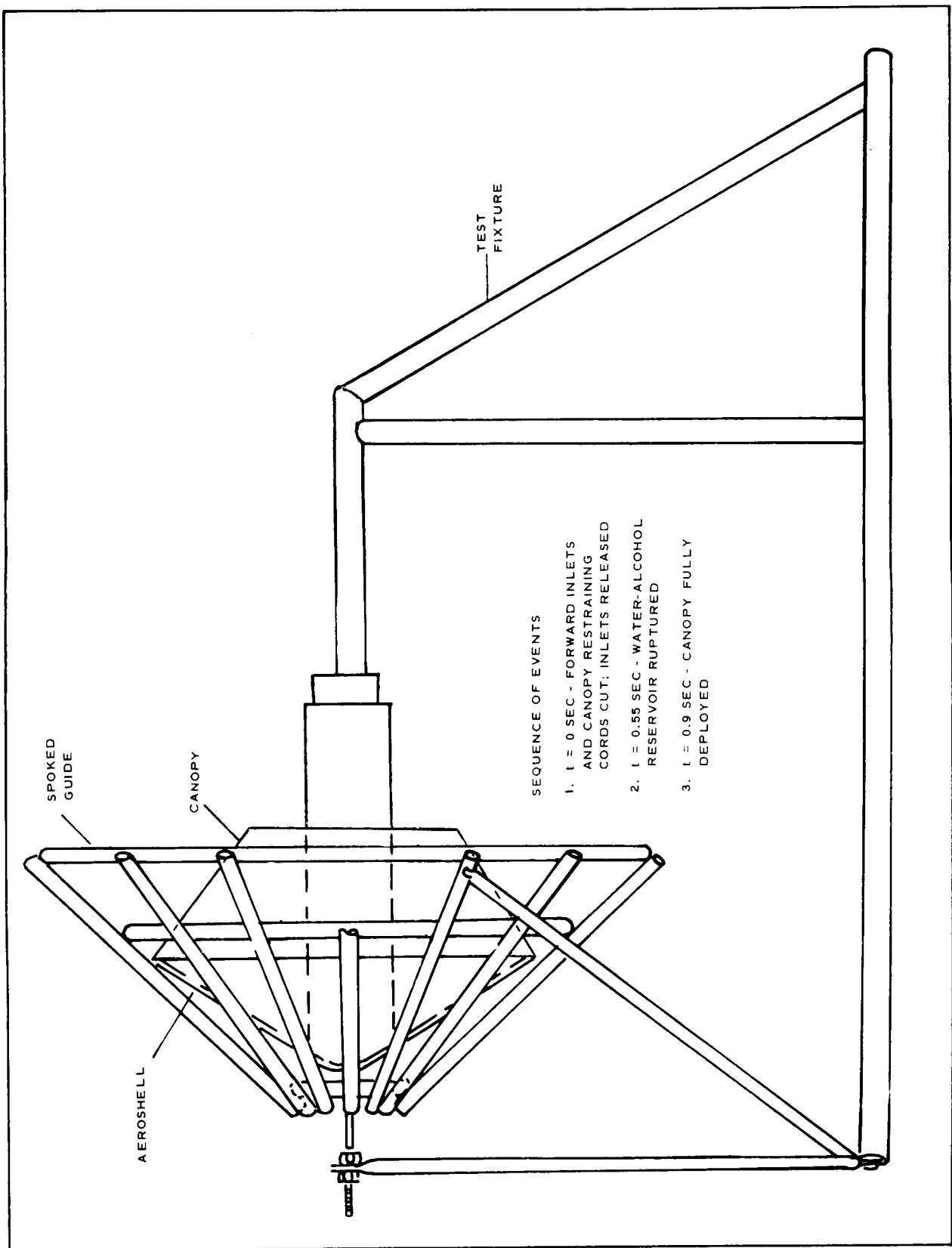


Figure 21. - Water-Alcohol Inflation Test Setup

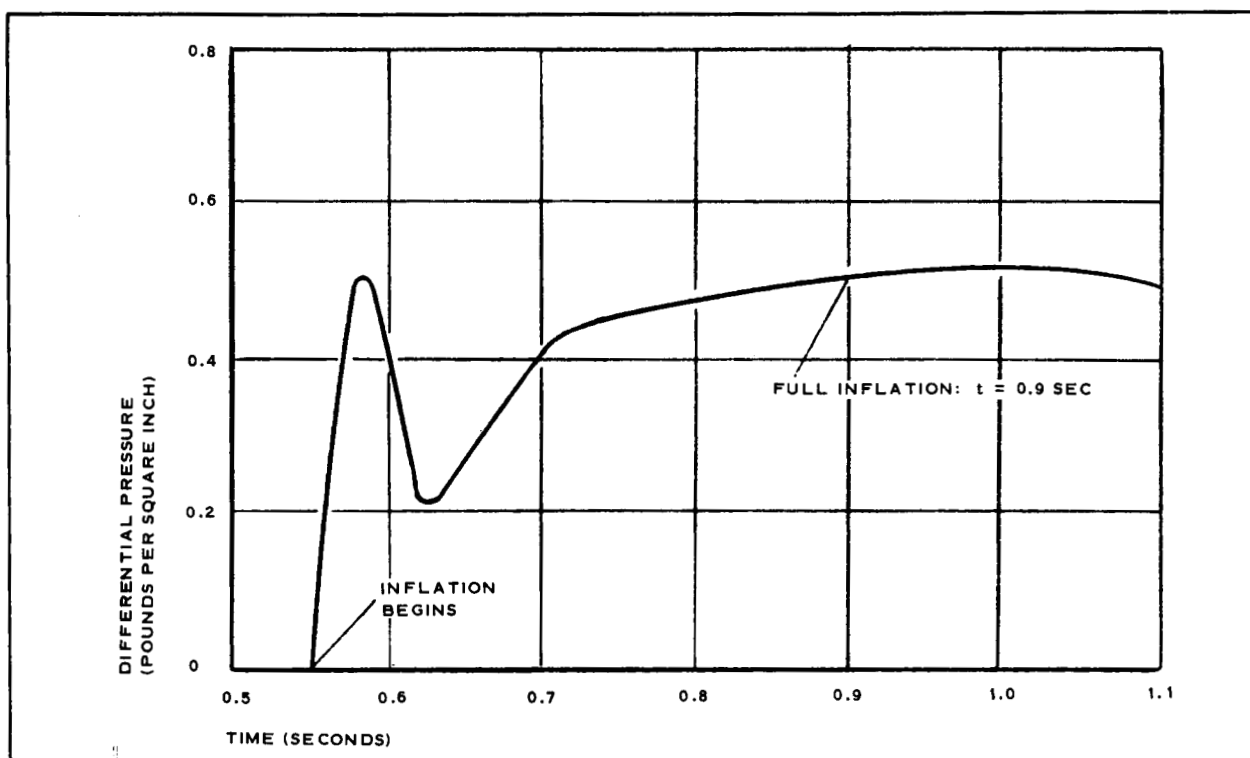


Figure 22. - AID Differential Pressure-Time History

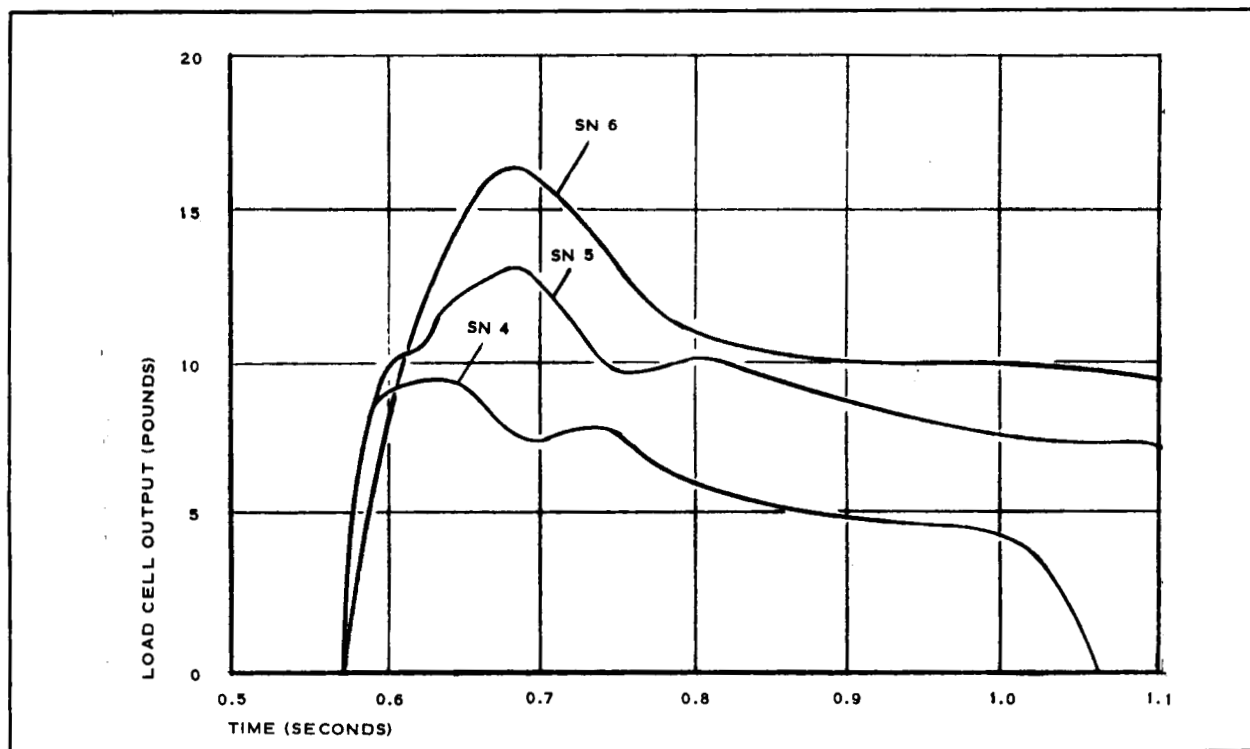


Figure 23. - Load Cell Force-Time History

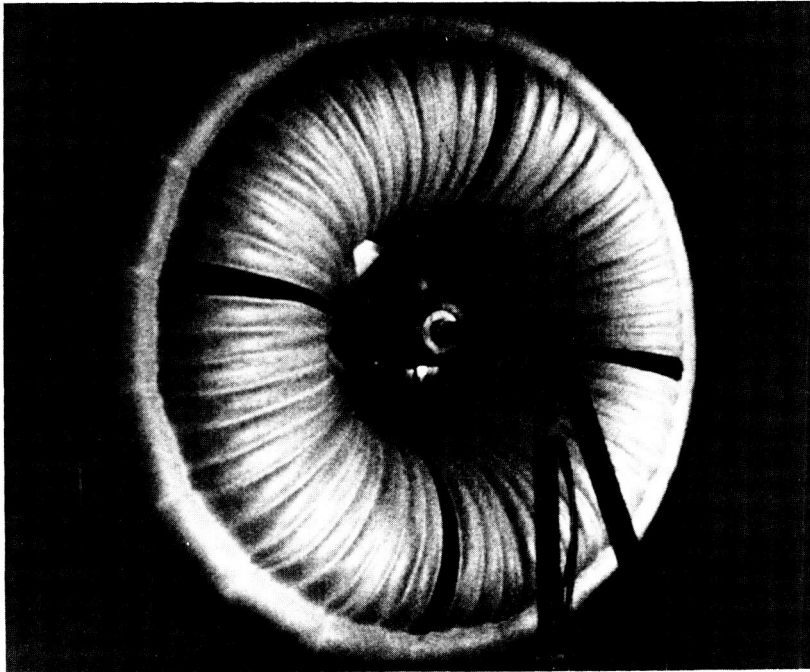


Figure 24. - Fully Inflated AID

APPENDIX A. - DRAWINGS

The working drawings for the attached inflatable decelerator system were generated by Goodyear Aerospace and are given below (see Figures A-1 through A-27).

1. Drawing 3063000-001: Attached Inflatable Decelerator System (5 sheets), 20 August 1970.
2. Drawing 3063000-002: Decelerator Assembly, Attached Inflatable (10 sheets), 20 August 1970.
3. Drawing 3063000-003: Support Ring Assembly and Aeroshell, Attached Inflatable Decelerator System (6 sheets), 20 July 1970.
4. Drawing 3063000-004: Support Assembly, Attached Inflatable Decelerator (4 sheets), 7 August 1970.
5. Drawing 3063000-110: Spring and Ring Assembly, Decelerator Assembly, Attached Inflatable (1 sheet), 9 October 1970.
6. Drawing 3063000-112: Tube Assembly, Decelerator Assembly (1 sheet), 23 February 1971.

1. IDENTIFY PER MIL-STD-130 (GAC PROCESS SPEC J2)

2. DRESS AEROSHELL SCREWS HEADS WITH DOW CORNING RTV-731 MIXED WITH 1 PART IN 10 OF ALUMINUM POWDER. PRIME SURFACE WITH DOW CORNING A-4094 PRIMER

3. BEND CANOPY END BANDS & POT HOLES FOR AIR SEAL WITH DOW CORNING RTV-731 ADHESIVE. WHEN USING ON METAL, PRIME WITH DOW CORNING A-4094 PRIMER

4. INSTALL INSERT PER MIL-SPEC MS33646 (GAC PROCESS SPEC M49)

5. MAKE MONEX TUBULAR BRAIDED CORD FROM 1200 DENIER 3/4" Z TWIST MONEX YARN AS FOLLOWS: 14 CARRIERS, 2 ENDS PER CARRIER, 72 PLIES PER INCH

6. TORQUE WITH MS3375 DRIVER, RECESS NO 4, TO 40 IN. LBS.

7. SOLDER 4 PLACES

8. REMOVE SHUNT (2 PLACES)

9. LINE CUTTER SCHEMATIC

10. EXCITATION POWER - (RETURN)

11. SIGNAL OUTPUT +

12. EXCITATION POWER + (10V MAX.)

13. SIGNAL OUTPUT - (RETURN)

14. CEC 4-3/16 PRESSURE TRANSDUCER & 4-019 ADAPTER SCHEMATIC

15. PARTS LIST

16. MATERIAL AND SIZE

17. ZONE

18. ITEM

19. FIND

20. NO.

21. REVISIONS

22. DATE

23. APPROVED

24. BY

25. ENGINEER

26. CUST.

27. 100-000996-001

28. SHEET 1 OF 5

Figure A-1. - Attached Inflatable Decelerator System
Drawing 3063000-001, Sheet 1

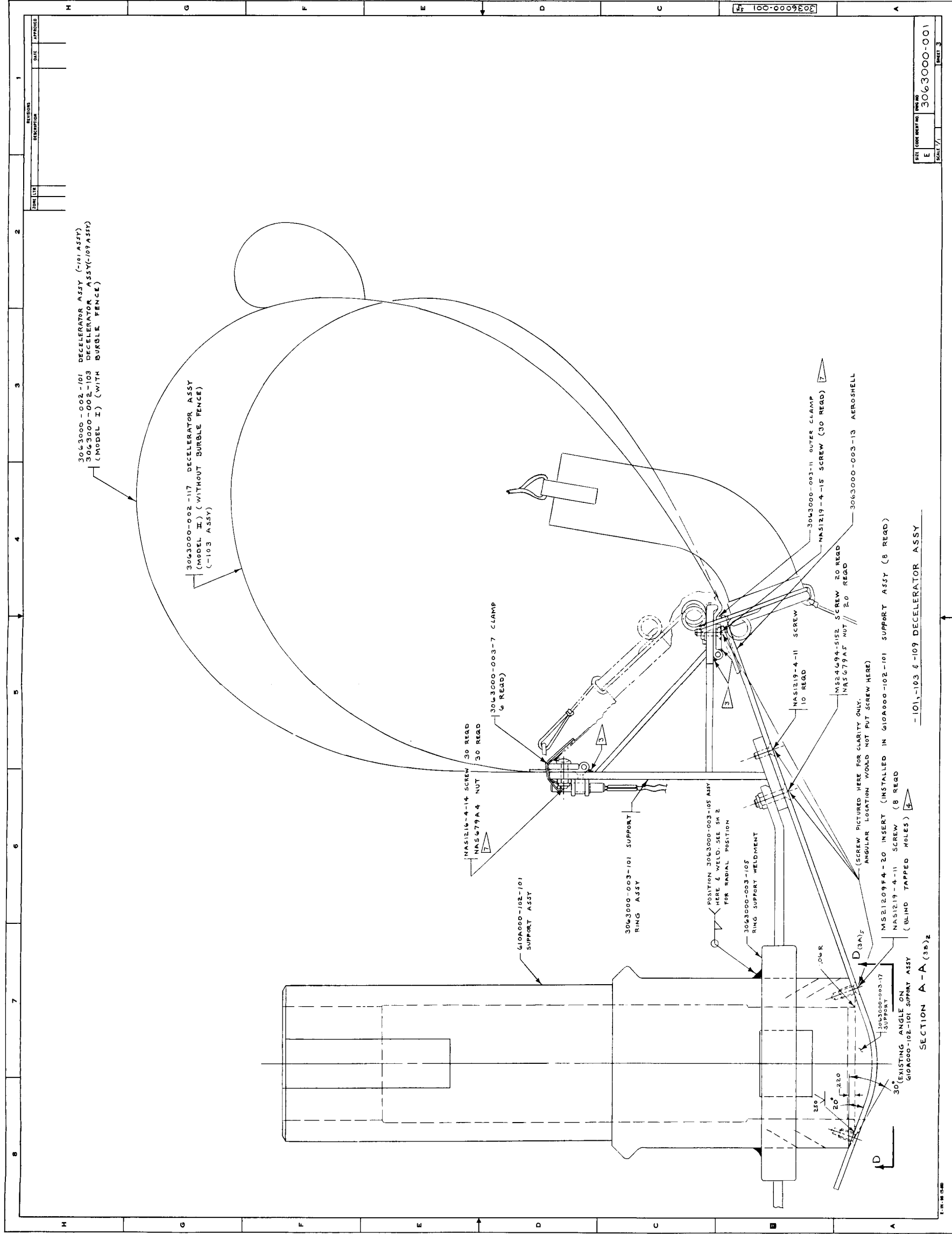


Figure A-3. - Attached Inflatable Decelerator System
Drawing 3063000-001, Sheet 3

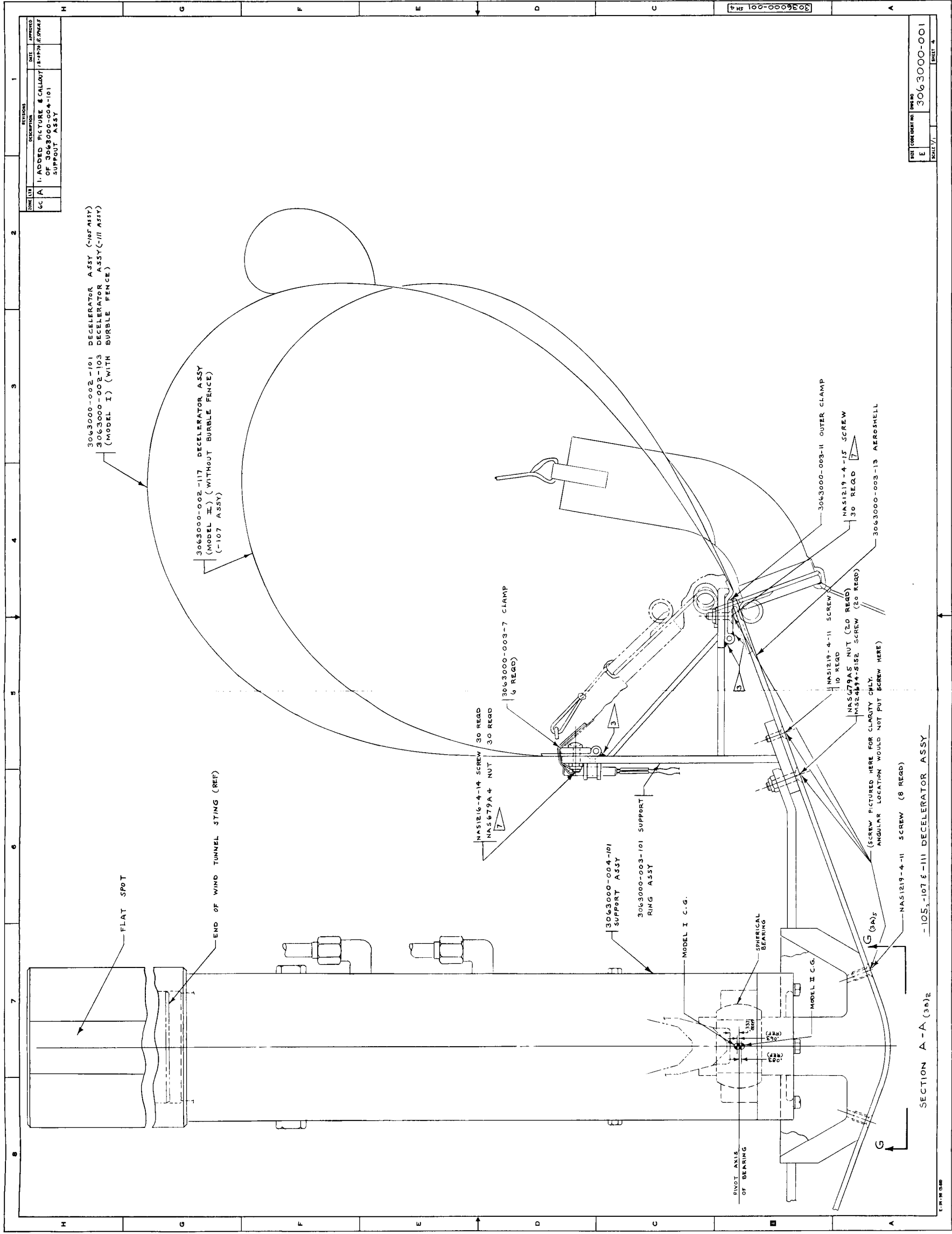
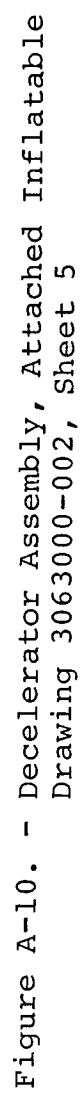
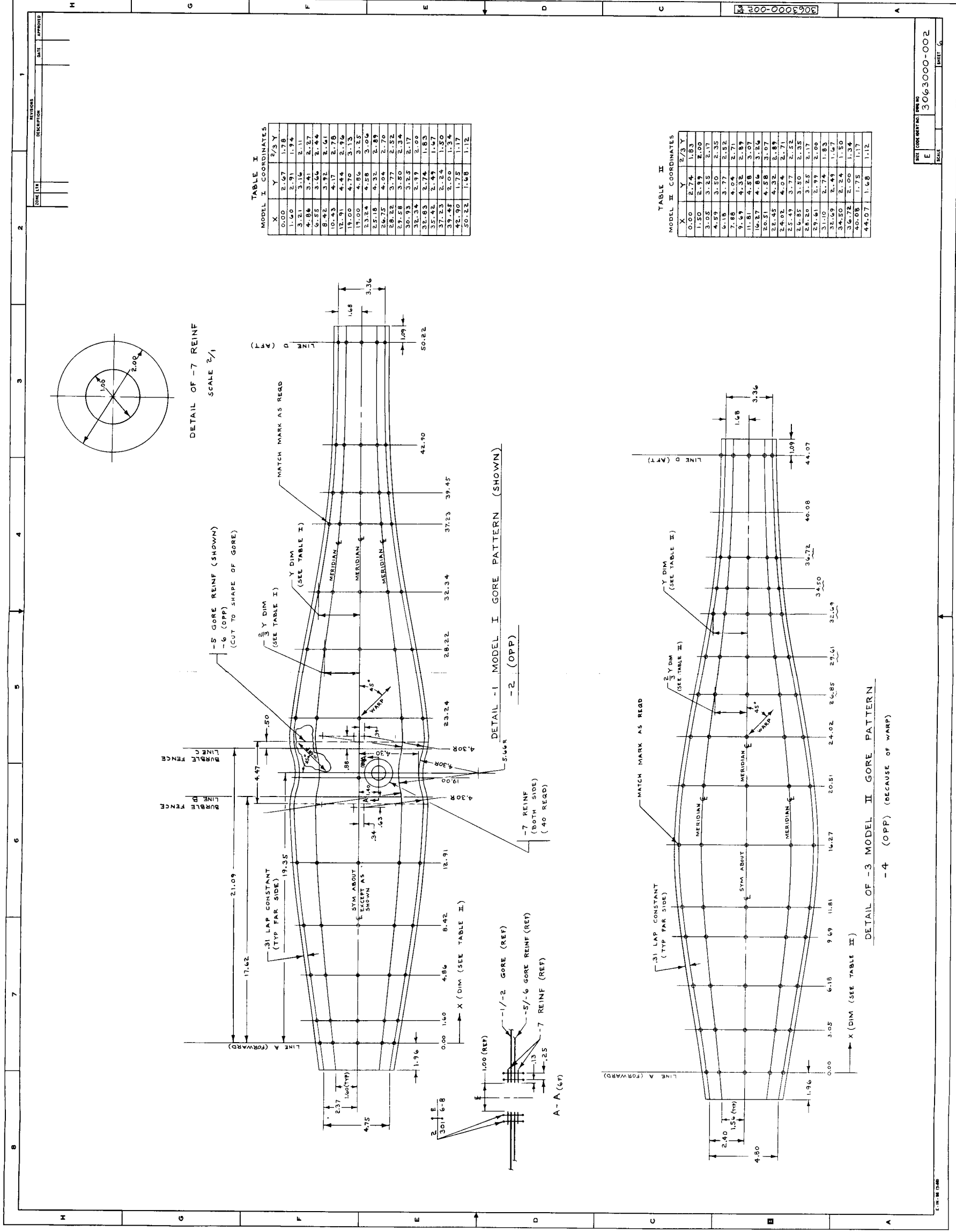


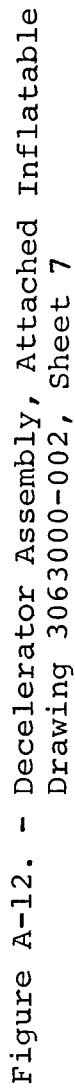
Figure A-4. - Attached Inflatable Decelerator System
Drawing 3063000-001, Sheet 4

[illegible]

Figure A-6. - Decelerator Assembly, Attached Inflatable
Drawing 3063000-002, Sheet 1







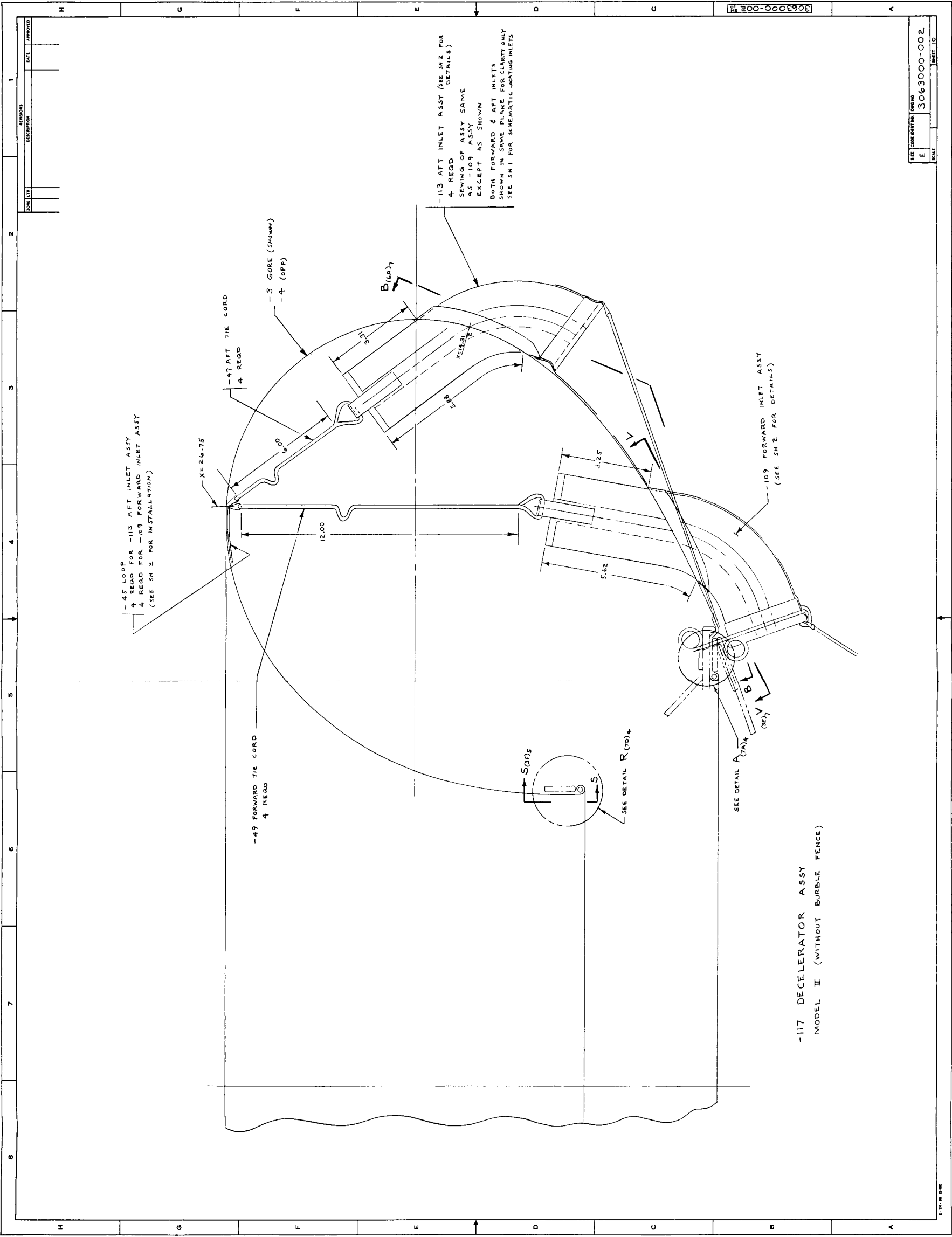


Figure A-15. - Decelerator Assembly, Attached Inflatable
Drawing 3063000-002, Sheet 10

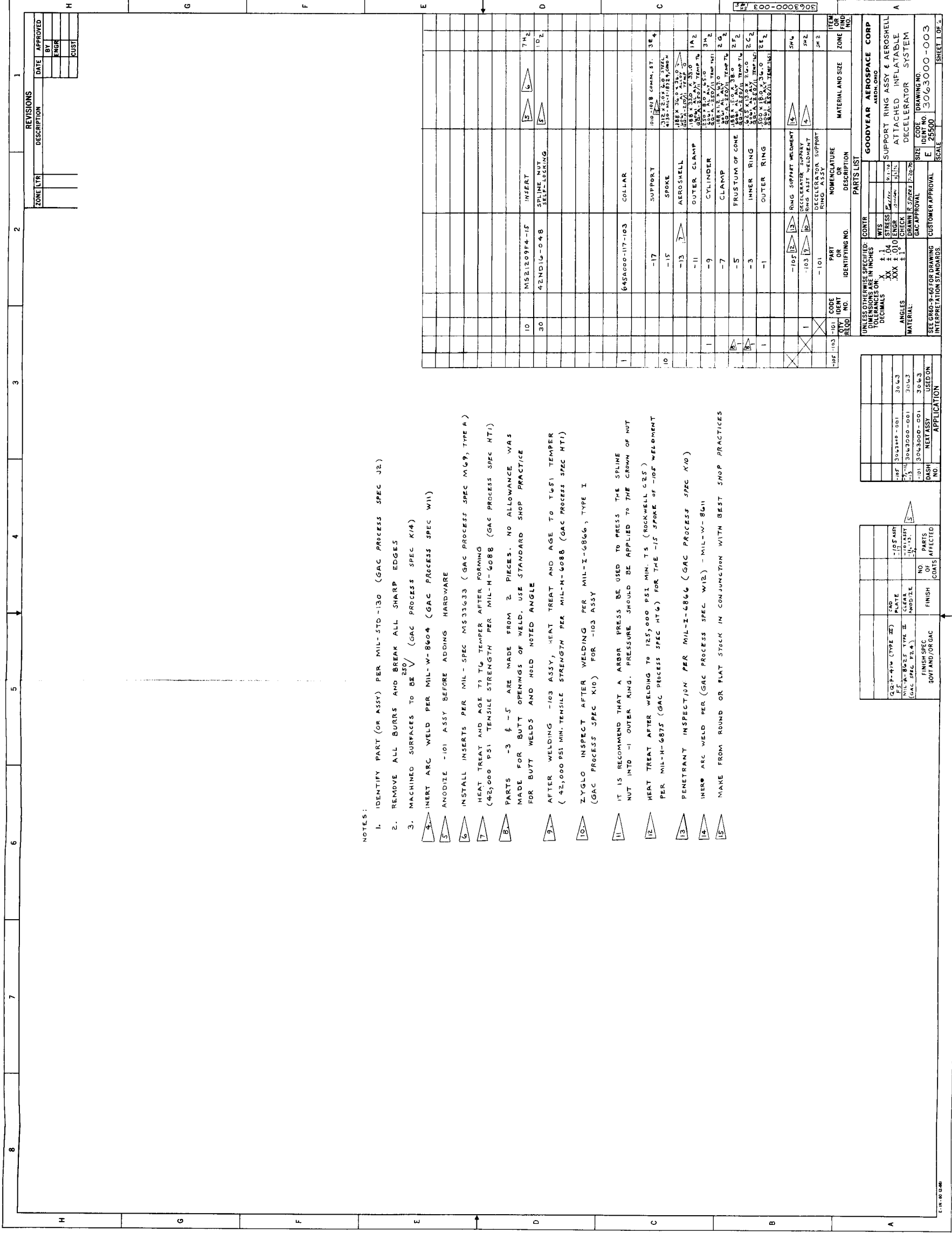
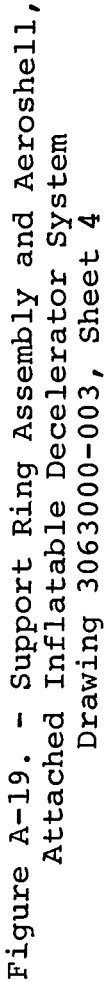


Figure A-16. - Support Ring Assembly and Aeroshell, Attached Inflatable Decelerator System Drawing 3063000-003, Sheet 1



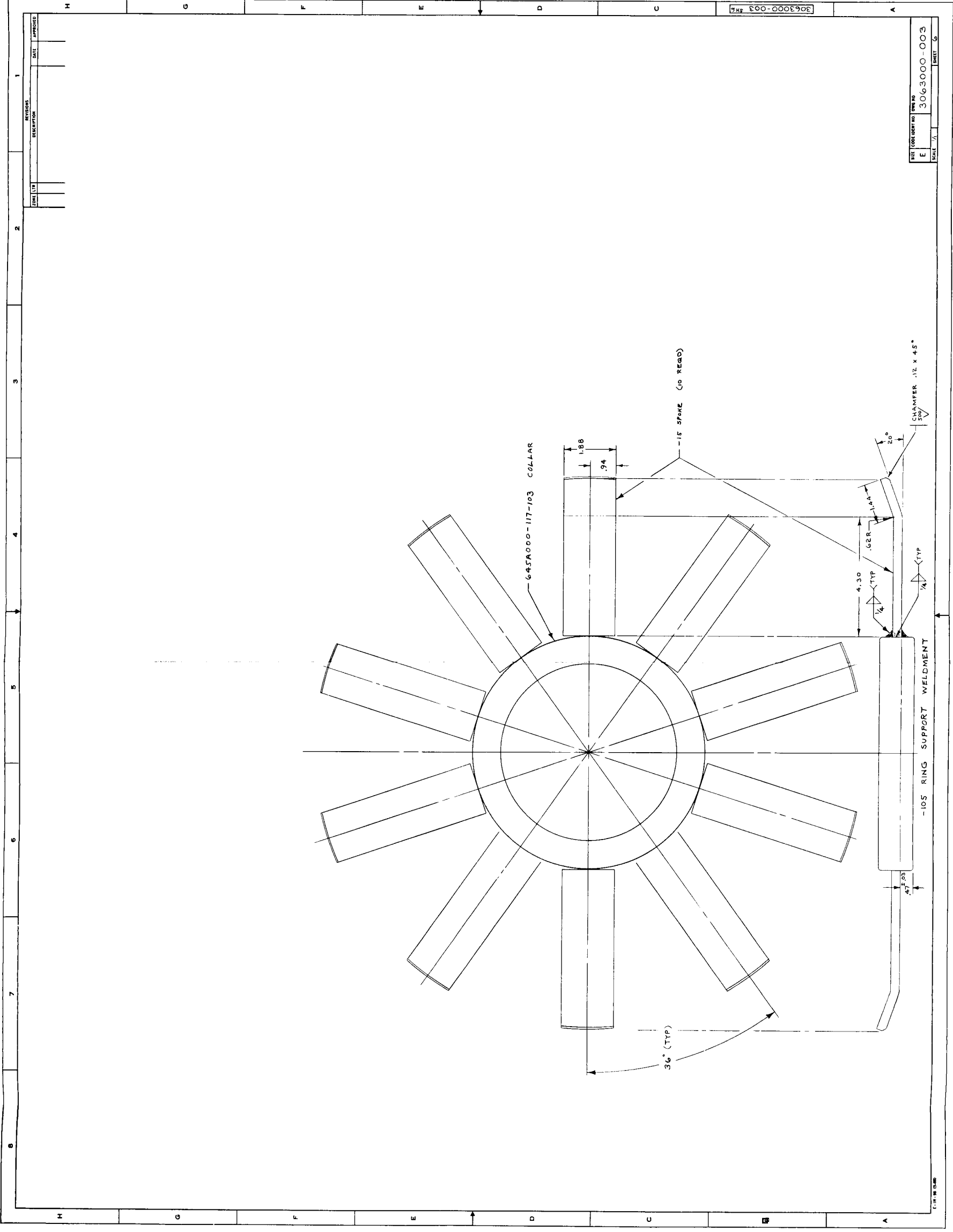


Figure A-21. - Support Ring Assembly and Aeroshell,
Attached Inflatable Decelerator System
Drawing 3063000-003, Sheet 6

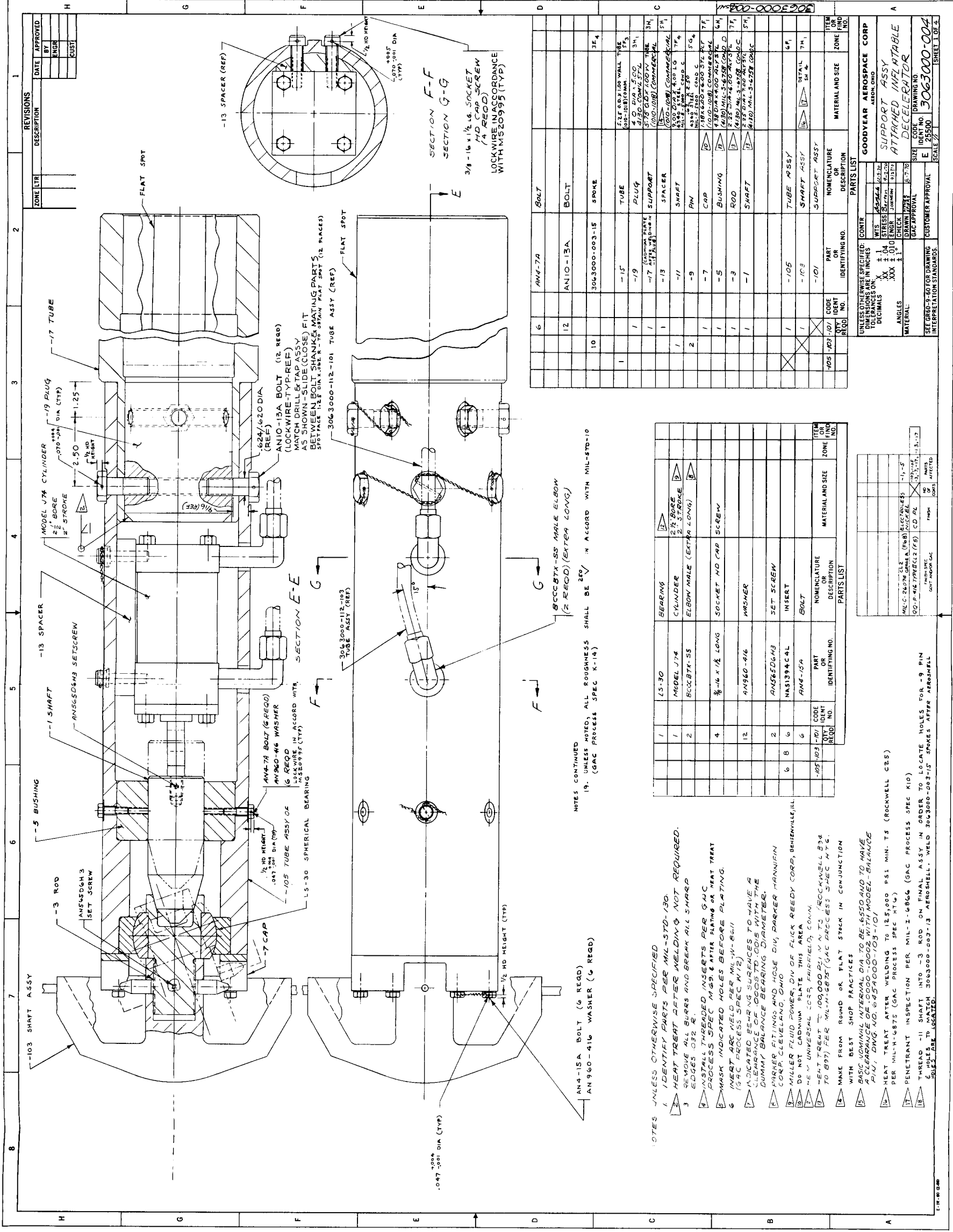


Figure 22. - Support Assembly, Attached Inflatable Decelerator Drawing 3063000-004, Sheet 1

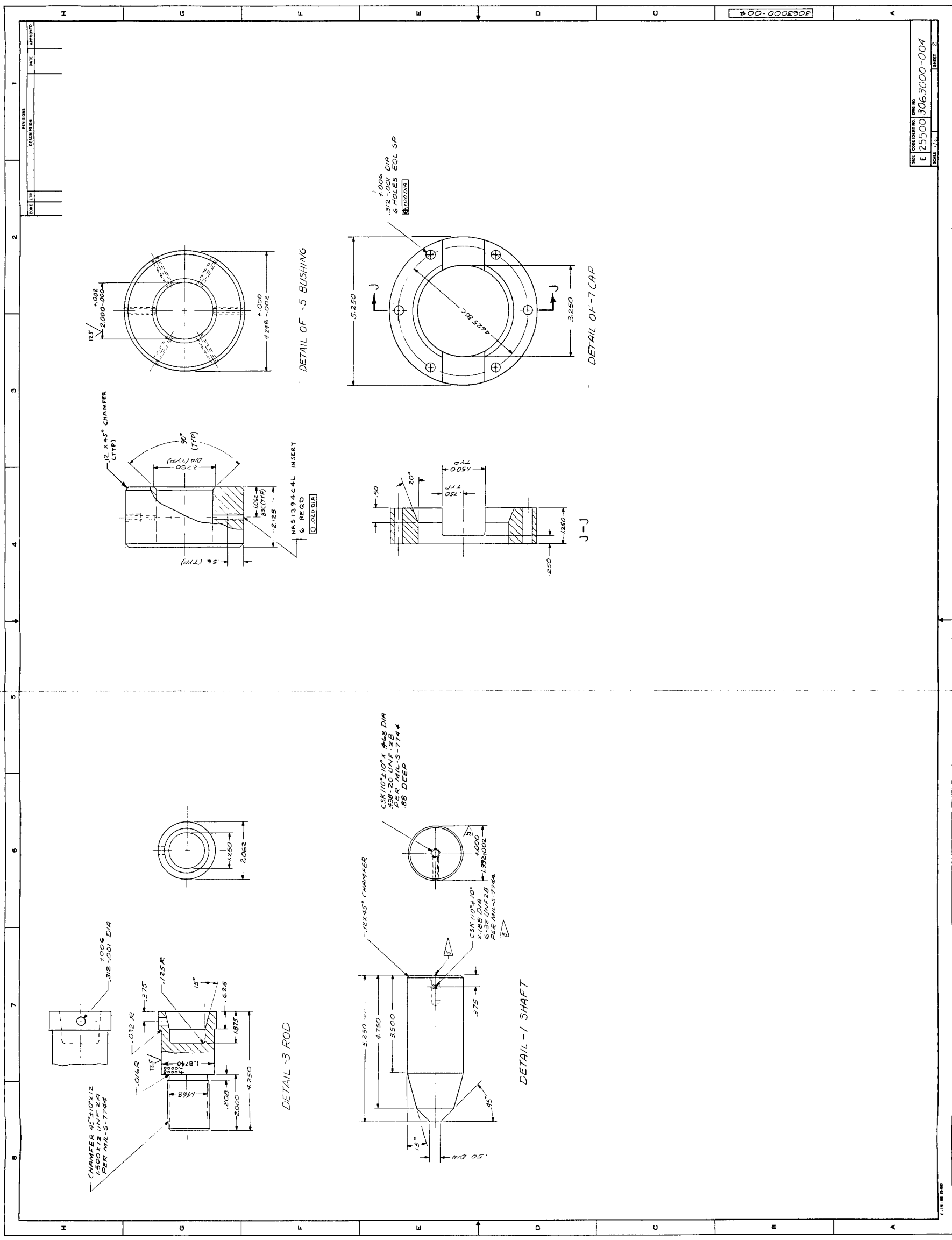
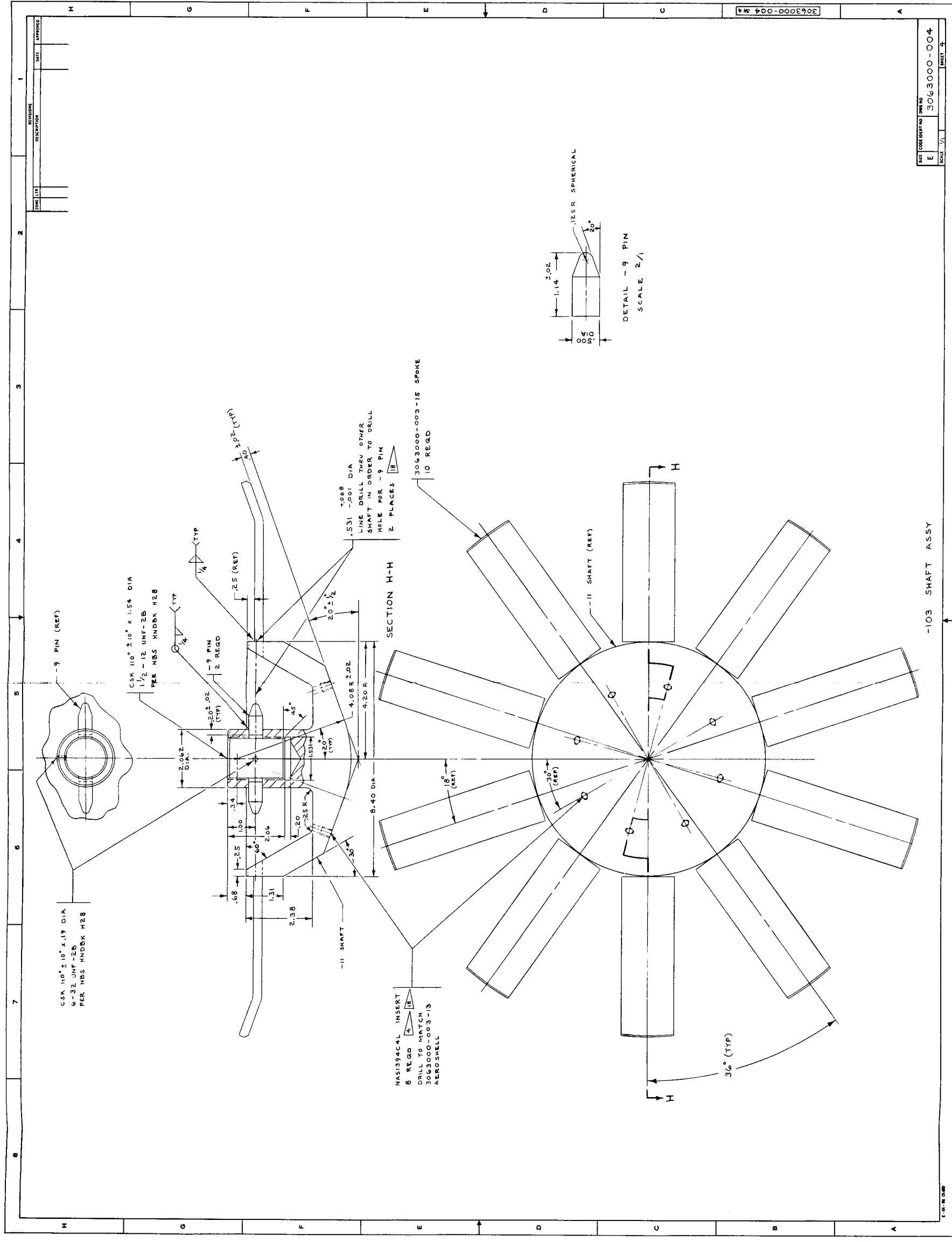


Figure 23. - Support Assembly,
Attached Inflatable Decelerator
Drawing 3063000-004, Sheet 2



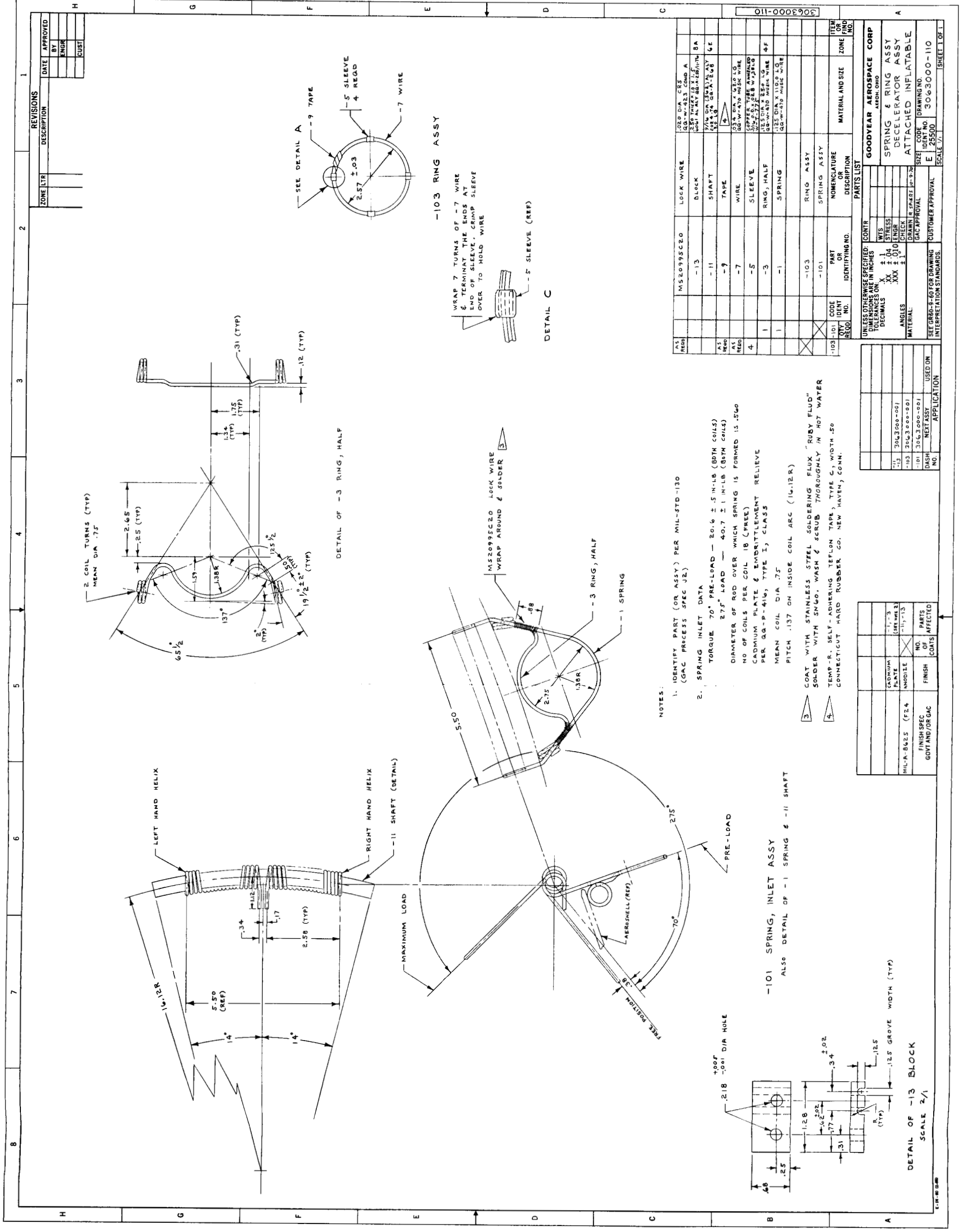


Figure 26. - Spring and Ring Assembly, Attached Inflatable Decelerator Assembly, Drawing 3063000-110, Sheet 1

APPENDIX B. - STRESS ANALYSIS

Fabric Stresses

A stress analysis was performed on model I only since the same materials were used in both configurations and model I had higher stress levels.

The decelerator stress analysis in Reference 1 presents the following relationships, based on the isotenoid method of analysis, for determining the limit loads for both the meridians and fabric. These relationships are:

$$N_B = \bar{N}_B \frac{pR}{2} \quad (B-1)$$

$$f_r = \bar{f}_r \frac{pR}{2} \quad (B-2)$$

$$f_f = \bar{f}_f \frac{pR}{2} \quad (B-3)$$

$$T_r = \bar{T}_r \frac{\pi p R^2}{n} \quad (B-4)$$

$$T_f = \bar{T}_f \frac{\pi p R^2}{n} \quad (B-5)$$

$$\bar{f}_f = \bar{f}_r + \gamma \bar{N}_B \quad (B-6)$$

$$\bar{T}_f = \bar{T}_r + (1 - \gamma) \bar{N}_B \quad (B-7)$$

From the data in Reference 6:

$$\frac{p}{q_\infty} = 1.9$$

For the maximum dynamic pressure of 200 psf given in Table II,

$$p = 1.9 (200)$$

$$= 380 \text{ psf}$$

$$= 2.64 \text{ psi}$$

Using the model parameters presented in Table III, the following limit loads were calculated:

APPENDIX C. - WEIGHT ANALYSIS

A weight analysis was performed to determine the weight of the AID models and their corresponding centers of gravity (cg). For the purpose of this analysis, the weight difference between the model I AIDS due to aft inlet size, which was 0.047 lb, was considered negligible and only the heavier model with larger aft inlets was used for cg computations.

The cg was calculated for both models I and II, packaged and deployed, and mounted and unmounted on the pivotal adapter. The last group of computations was performed to determine the cg of the models relative to the pivot axis of the pivotal adapter. A design goal of the program was to have the cg as near the pivot axis as possible in order to reduce model unbalance effects when the locking pin is released during wind tunnel tests.

The reference datum used in these calculations was the base plane of the aeroshell as shown in Figures C-1 and C-2. Figure C-1 also shows the relative position of the pivot axis to the base plane of the aeroshell. Positive moments are aft of the base plane and negative moments are forward of the base plane.

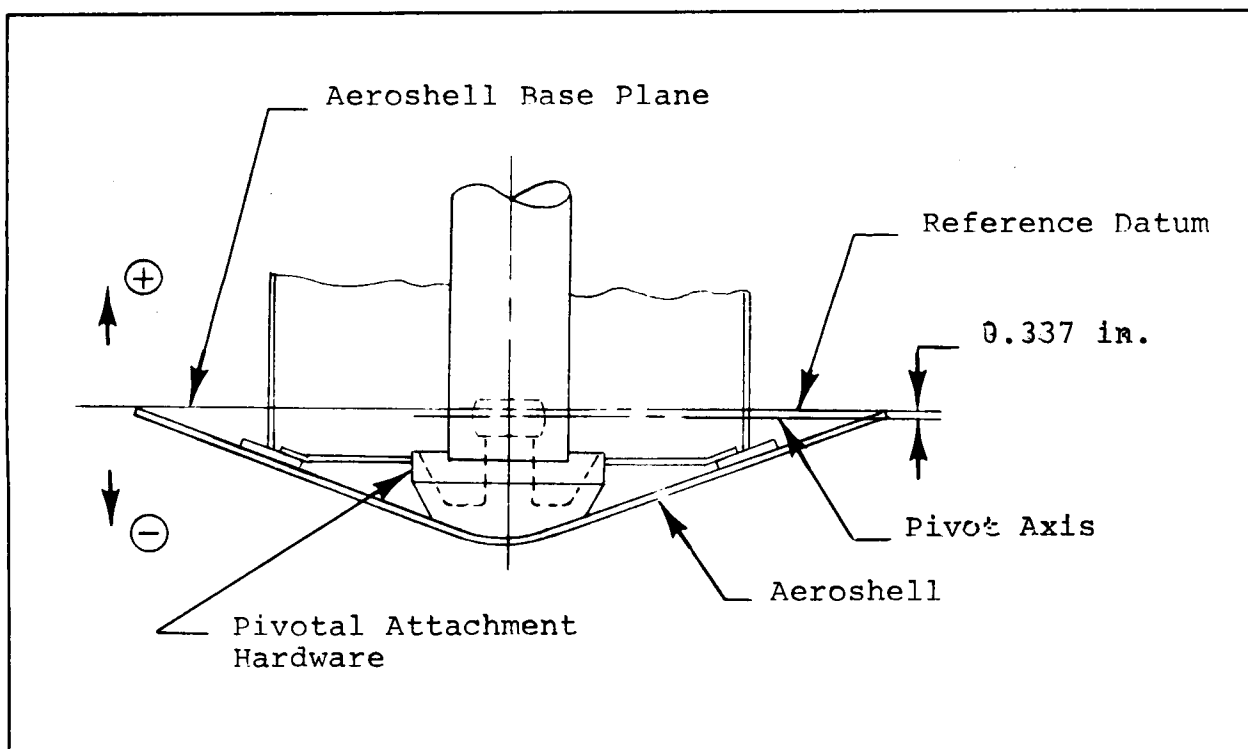


Figure C-1. - Reference Datum for AID Models Mounted on Pivotal Adapter

The canopy weight includes all the fabric, inlets and inlet rings, inlet restraining lines, and load cells. The spring weight includes only the weight of the four forward inlet springs. The aeroshell weight is only that of the aeroshell. The hard structure weight includes all internal supports and structure, clamps, cutters, attachment fittings and screws, nuts, and bolts. The total weight of the model is the weight of the whole AID before attachment to the support sleeve but including the weight of the attachment nuts, bolts and screws. The pivotal attachment hardware weight includes that of the rod and threaded shaft and solid shaft. The total model weight on the pivotal adapter is the weight which must be supported by the pivotal adapter bearing.

The cg locations calculated for models I and II are presented in Table C-II.

TABLE C-II. AID MODELS CENTER OF GRAVITY LOCATIONS

Model	Center of Gravity Location (in.)			
	Model Without Support		Model with Pivotal Attachments	
	Packaged	Deployed	Packaged	Deployed
I	0.391	0.651	-0.533	-0.274
II	0.370	0.477	-0.588	-0.420

REFERENCES

1. Bohon, H. L.; and Miserentino, R.: Attached Inflatable Decelerator Performance Evaluation and Mission-Application Study. AIAA Paper No. 70-1163, AIAA Aerodynamic Deceleration Systems Conference (Dayton, Ohio), September 1970.
2. Mikulas, M. M., Jr.; and Bohon, H. L.: Summary of the Development Status of Attached Inflatable Decelerators. AIAA Paper No. 68-929, AIAA Second Aerodynamic Decelerator Systems Conference (El Centro, California), September 1968.
3. Barton, R. R.: Development of Attached Inflatable Decelerators for Supersonic Application. NASA CR-66613, 1968.
4. Houtz, N.: Optimization of Inflatable Drag Devices by Isotensoid Design. AIAA Paper No. 64-437, First Annual AIAA Meeting (Washington, D. C.). 29 June through 2 July 1964.
5. Baker, D. C.: Investigation of an Inflatable Decelerator Attached to a 120-Deg Conical Entry Capsule at Mach Numbers from 2.55 to 4.40. AEDC-TR-68-227, U. S. Air Force, October 1968.
6. Baker, D. C.: Investigation of an Attached Inflatable Decelerator with Mechanically Deployed Inlets at Mach Numbers from 2.25 to 4.75. AEDC-TR-69-132, U. S. Air Force, June 1969.
7. Reichenau, David E. A.: Investigation of an Attached Inflatable Decelerator System for Drag Augmentation of the Voyager Entry Capsule at Supersonic Speeds. AEDC-TR-68-71, U. S. Air Force, April 1968.
8. Bohon, Herman L., and Miserentino, R.: Deployment and Performance Characteristics of 5-Foot-Diameter Attached Inflatable Decelerators from Mach Number 2.2 to 4.4. NASA TND-5840, August 1970.
9. Faurote, G. L.: Design, Fabrication, and Static Testing of Attached Inflatable Decelerator (AID) Models. NASA CR 111831, 1 March 1971.
10. Baker, D. C.: Performance Evaluation of Attached Inflatable Decelerators with Mechanically Deployed Inlets at Mach Numbers from 2.6 to 4.4. AEDC-TR-70-254, U. S. Air Force, November 1970.
11. Gillis, C. L.: Aerodynamic Deceleration Systems for Space Missions. AIAA Paper No. 68-1081, AIAA Fifth Annual Meeting (Philadelphia, Pa.), October 1968.